A SEARCH FOR PERIODIC STRUCTURE IN SOLAR 2 CM MICROWAVE RADIATION

by

Davis D. Sentman

Research was sponsored in part by the Office of Naval Research under contract N00014-68-A-0196-0003.

Department of Physics and Astronomy
THE UNIVERSITY OF IOWA
Iowa City, Iowa 52242

U. of Iowa 73-20

A SEARCH FOR PERIODIC STRUCTURE IN SOLAR 2 CM MICROWAVE RADIATION

by

Davis D. Sentman

A thesis submitted in partial fulfillment of the
requirements for the degree of Master of Science
in the Department of Physics and Astronomy
in the Graduate College of
The University of Iowa

May, 1973

Thesis supervisor: Assistant Professor Stanley D. Shawhan

This research was supported in part by the National Aeronuatics and Space Administration under grant NGL-16-001-002, and by the Office of Naval Research through contract N00014-68-A-0196-0003.

ABSTRACT

Two hundred and eighty-five hours of solar data obtained from the University of Iowa 2 cm radiometer during 1968—1969 were analyzed for evidence of the 5 min periodic chromospheric oscillations. A power spectral analysis of the data failed to show any statistically significant ($> 96\%$ confidence) periodic activity in the frequency range 1—15 mHz. No correlation was found between 2 cm periodicities and other forms of solar activity at several different chromospheric heights in H_α, soft solar x rays (2—12 Å), and several microwave frequencies (3—15 GHz).

A small shift in power from low to higher frequencies in the power spectrum of the 2 cm data was found to be correlated with H_α and x-ray activity. This power shift is attributed to a relative increase in chromospheric turbulence at altitudes common to H_α, x-ray and 2 cm emission.

A statistical analysis of previous works reporting evidence for the oscillations at microwave frequencies indicates that confidence in these previous results is marginal.

A model for chromospheric oscillation bursts in quiescent supergranules deduced from Bhattacharyya (1972) is presented. The model is an exponentially damped wave train burst with a 15 min mean damping time and a mean burst period of 50 min. Using the statistical

properties of power spectra, an expression for the minimum detectable signal-to-noise ratio is derived and applied to the model using the most significant results of experiments to date to yield:

(1) an estimate of $\sim 1.5 \times 10^{-3}$ as the upper limit for the ratio of the oscillation mean peak-to-peak to ambient temperature at chromospheric heights,

(2) an estimate of ~ 0.02 as the upper limit for the mean fraction of the quiescent solar surface experiencing oscillations, and

(3) estimates for the minimum amount of data required for confident detection of the periodicities. In an ideal experiment utilizing the NRAO Kitt Peak 36 ft antenna at a wavelength of 1 mm and assuming the present model for oscillation bursts and reasonable equipment and data parameters, ~ 1.25 hr of data are calculated to be the least amount required.

I. INTRODUCTION

The existence of characteristic oscillations in the solar atmosphere has been known for some time. Following the first theoretical treatment of the problem by Whitney (1958) the experimental verification of the 5 min period oscillations was reported by Leighton et al. (1962) using a Doppler spectroheliograph technique. A short time later Evans and Mitchard (1962) and Howard (1962) extended the observational techniques of detecting the periodicities by using, respectively, time series analysis of high dispersion spectra and photoelectric detection. Since that time many investigators have succeeded in extending the range of optical observations using a variety of techniques over a wide range of spectral frequencies. Noyes (1967) gives a comprehensive summary of early observations and the discovery of the solar supergranulation and its relation to the chromospheric network, and reviews the geometrical model which resulted from those observations.

An important finding was that the oscillations existed at heights in the solar atmosphere extending into the lower chromosphere. Generally speaking a peak in the velocity spectrum occurred at a period of about 300 sec for spectral lines corresponding to low photospheric altitudes and moved toward shorter periods as observations were made at higher altitudes (Noyes and Leighton, 1963). The intensity

spectrum followed the velocity spectrum closely, though it was more pronounced at high photospheric altitudes where the atmosphere is nearly adiabatic than at low photospheric altitudes where it is nearly isothermal (Noyes and Leighton, 1963). The observation of the oscillations in the H_α velocity spectrum (Elliot, 1969) and in the H_α intensity spectrum (Bhatnagar and Tanaka, 1972) showed that the oscillations persist to heights characteristic of H_α line formation, on the order of 5×10^3 km. Since this is in the neighborhood of the region where millimetric and centimetric radiation are observed to originate it is reasonable to ask whether or not the observed fluxes at these radio frequencies are modulated by the pressure fluctuations associated with the oscillations.

Reported radio observations of the oscillations have been far fewer in number than optical observations. Yudin (1968) reported having observed the 5 min period intensity modulation of 3.3 cm radiation. This same period, along with several other components, was also reported by Durasova et al. (1971) at the same frequency and apparently by using the same instrument. Simon and Shimabukuro (1971) found an oscillatory component at 5.6 mHz corresponding to a period of 180 sec, in their study of 3.3 and 3.5 mm solar data. Longer period components of from 30 to 60 min were investigated by Kobrin and Korshunov (1972) at a wavelength of 3.1 cm and by Kauffman (1972) at 4.3 cm. Gotwols (1971) showed that short period oscillations can exist after flares in the decimetric wavelength region.

Establishing the degree to which the oscillatory phenomenon exists at chromospheric and higher altitudes is important for a number of reasons, perhaps chief among which is determining how large a role it plays in heating the solar corona. A search was instituted for periodicities in the range 1—15 mHz using data taken in 1968—1969 on the University of Iowa 2 cm radiometer. The results of the search and a review of the findings of others, with particular emphasis given to the statistical aspects of the resulting power spectra, are the subject of this thesis.

Section II describes the equipment used to gather the data and the data reduction and digitization procedures. The data activity classification scheme and power spectrum analysis are described in section III. Section IV is devoted to a discussion of the results of the power spectrum analysis. The absence of detectable periodicities is compared with the findings of others and an attempt is made to assess the statistical reliability of the respective results. Several statistical parameters related to the power spectrum detectability of a signal embedded in noise are derived in section V. These parameters are applied to an oscillation burst model to yield upper limit estimates for oscillation amplitudes and the mean fraction of surface area experiencing oscillations in the quiescent solar atmosphere.

II. EQUIPMENT DESCRIPTION AND DATA HANDLING

Data used for this study were recorded from the 2 cm radiometer operated by the University of Iowa at the North Liberty Radio Observatory (NLRO) (Wende, 1969). The system has a 4 ft diameter, equatorially-mounted aluminum paraboloid equipped with a dual linear polarized Cassegrain feed. The antenna half-power beamwidth is 1° so the entire sun is viewed. The receiver operates at a center frequency of 15.375 GHz with an IF bandwidth of 20 MHz.

The radiometer is of the Ryle-Vonberg type. Antenna noise is balanced against the noise from a gas discharge tube-precision attenuator, resulting in a stability dependent only upon the gas discharge tube stability. The servo motor is driven at 100 pps, yielding a 10 msec response time for a 4 K change in antenna temperature. A potentiometer is connected to the servo motor shaft, providing an output voltage according to the position of the attenuator. This output voltage is used to drive a voltage controlled oscillator (VCO). For a more complete description of the system see Wende (1968, 1969) and Collins (1967).

During operation the radiometer was calibrated daily using a procedure which entailed inserting a known servo error voltage from a precision potentiometer. From the manufacturer's calibration curves one could then determine the calibration curve of the antenna temperature T_A versus the VCO frequency as shown in Figure 2.

The VCO output was recorded on magnetic tape along with a WWV calibrated, 1 kHz NASA 36-bit time code timing reference. The recorded timing reference was later used to trigger the A/D digitizing equipment and provided an absolute standard against which to measure the integrated VCO frequency. It was thus insured that any effects due to wow and flutter present in either the recording or playback systems were effectively compensated for.

A/D conversion was carried out by separating the magnetic source tape output into its time code and data components and using the time code reference to control the data sampling system, as represented schematically in Figure 3. The sampling system had a maximum time resolution of 100 msec and basically consisted of a frequency counter with a time base set equal to the desired sample period, which in this case was 5 sec. The output from this system therefore represented a 5 sec integrated average of the radiometer VCO frequency. Integrated samples were recorded sequentially on paper tape. One time sync was also punched every 10 min, containing the start time of the 10 min period, sampling period, and supplemental information (such as weather information for that data day) that could be coded into the system by means of switches on the front of the sampling system. The digitized, integrated VCO frequency samples were converted to antenna temperature by means of the calibration curve in Figure 2 and stored on magnetic tape for later computer analysis. Extensive checks were made during the conversion process to detect

spurious data points which were replaced by values interpolated from good points on either side. The fraction of data points that had to be corrected in this way was less than 0.01 for the entire set of digitized data and is estimated to be less than 0.002 for the data selected for power spectrum analysis.

Estimates can be made for the receiver noise (Krauss, 1966) and the effective temperature resolution of the system.

For the receiver noise

$$\frac{\Delta T_r}{T_s} = \frac{1}{\sqrt{B\,\Delta\tau}}$$

where

ΔT_r = rms receiver noise,

T_s = system temperature

$= T_A + [(10 \log_{10} NF) - 1]\, T_o$,

T_A = antenna temperature,

NF = system noise figure $\approx$ 11 Db,

T_o = ambient temperature $\approx$ 300 K,

B = receiver bandwidth = 20 MHz, and

$\Delta\tau$ = sample integration time.

For a typical day $T_A \approx$ 1000 K. In order to achieve a reasonable compromise between statistical reliability and frequency resolution of the computed power spectra $\Delta\tau$ was chosen to be 30 sec. The

5 sec integrated T_A averages were therefore averaged in groups of six to yield an effective data sampling period and integration time of 30 sec. These parameters then give a system noise of $\Delta T_r \approx 0.16$ K.

Although the stepping resolution of the system is approximately 4 K, for a noisy signal with an rms deviation appreciably larger than this the effective temperature resolution of the system for a sample period of $\Delta\tau$ is given by

$$\Delta T_{eff} = \frac{\Delta T_{step}}{\sqrt{f_{step} \cdot \Delta\tau}}$$

where

ΔT_{eff} = effective stepping resolution, K;

ΔT_{step} = system stepping resolution, K;

f_{step} = stepping frequency = 100 Hz; and

$\Delta\tau$ = data sample period = 30 sec.

Hence $\Delta T_{eff} \approx 0.07$ K.

There is an additional source of noise due to the uncertainty of the sampling system frequency counter of ± 1 count per data sample. For a VCO frequency of 600 Hz ($T_A \approx 1000$ K) this results in an uncertainty of 1/3000, and for six averaged 5 sec samples corresponds to a probable error factor of $(1/3000) \times (1/\sqrt{6}) = 1.5 \times 10^{-4}$. From Figure 2, this factor corresponds to $\Delta T_A \approx 2$ K.

Thus the largest source of artificially-generated noise in the reduced antenna temperature data is due to that introduced by

the digitization process. However the rms noise of the quiescent sun about the mean at any given time is observed to be on the order of 10—20 K for a data sample integration time of 30 sec, or nearly an order of magnitude larger than ΔT_A. We therefore conclude that all but a small fraction of the noise present in a plot of T_A versus time is true solar centimetric noise.

III. DATA ANALYSIS

Of the more than 200 days of data taken during 1968—1969, 40 days, representing those of the best quality, were selected for study. The criteria for selection were that the data must be free of discontinuities and irregularities, weather conditions must be clear, and a minimum of 4 h of continuous data must exist in a given record. For a given day records as long as possible were chosen to be free of any large flares that might force the data to depart significantly from stationarity, though no attempt was made to choose data completely free of all activity. The total amount of data represented in all records was greater than 285 h, making the average record length about 7 h. The 5 sec data samples were averaged in groups of six to yield samples corresponding to 30 sec integrated antenna temperature averages. A typical day of data with 30 sec time resolution is shown in Figure 4.

The standard Blackman-Tukey (1958) algorithm with Hamming smoothing was used to compute the power spectrum for each data record. The maximum lag M in the autocorrelation function was set at 25 min for each record so that all of the individual spectra have the same frequency resolution $\Delta f = 1/2M$. Because of the large amount of power present at low frequencies the data was pre-whitened prior to computation to prevent the low-frequency power from leaking to higher

frequencies via the side lobes in the spectral window. This was accomplished by means of a digital high-pass filter constructed as follows.

For n successive passes through the data with the elementary low-pass filter function

$$\langle x_i \rangle = \frac{1}{2} x_i + \frac{1}{4} (x_{i-1} + x_{i+1}) \quad ,$$

Holloway (1958) showed that the power transfer function is

$$R(f) = \cos^{2n}(\pi f \Delta\tau) \quad .$$

If the resulting smoothed data is subtracted from the original unsmoothed data set the difference represents the original data filtered by a high-pass filter with a power transfer function equal to the complement of R(f),

$$R'(f) = 1 - R(f) \quad .$$

The antenna temperature data were filtered using this technique with n = 10. The resulting transfer functions R(f) and R′(f) are plotted in Figure 5 . After pre-whitening was completed the data were normalized to zero mean and unit standard deviation and the power

spectrum computed. Post-darkening was then applied to the power spectrum by multiplying by the inverse of $R'(F)$ to complete the calculation. Examples of the resultant power spectra, normalized to a value of 10 in the interval 4—5 mHz for display purposes, are shown in Figures 6 and 7.

The statistical accuracy of the computed spectra is estimated in terms of equivalent degrees of freedom and their associated confidence limits. For a one-dimensional time series for which the power spectrum is computed using the Blackman-Tukey (mean-lagged-product) method the degrees of freedom, which may be thought of as representing the number of estimates of power in the frequency interval $\Delta f = 1/2M$, are given by (Blackman and Tukey, 1958)

$$k = 2\left(\frac{T}{M} - \frac{1}{3}\right)$$

where

k = degrees of freedom,

T = length of data set under consideration, and

M = maximum lag in the autocorrelation function.

A measure of the probability that an estimate falls within an upper and lower bound, the ratio of which is designated the confidence factor, is given by

$$f_{conf} = 10^{b/(10\sqrt{k-1})} = \exp\left(\frac{2.3\ b}{10\sqrt{k-1}}\right)$$

where

f_{conf} = confidence factor for a given confidence;

k = degrees of freedom; and

b = factor depending on desired confidence, given as follows:

	confidence				
	50%	80%	90%	96%	98%
b	8	16	20	25	29

This is an approximation, but for $k \geq 4$ is very close to more exact calculations based upon chi-square tables (Edmonds, 1966). In this study the least figure for k was 18.5, obtained for three of the records.

It must be emphasized that no study of power spectra can be considered reliable or complete without the inclusion of an error analysis, particularly in cases where the signal-to-noise ratio is very poor and the peaks in the calculated power spectra are nominal. This must be true no matter how the power spectrum is computed, for the confidence limits are merely an expression of the uncertainty principle applied to the analysis of a time series.

Of the 40 power spectra computed, one for each record, only one, shown in Figure 8, showed any evidence of having a statistically

significant periodicity present. The remaining spectra all showed structure that fell well within the confidence limits. This result was not unexpected, for the large antenna beamwidth included the entire disc of the sun in its pattern. Unless there were several exceptionally strong coherent sources, or alternately, adjacent regions on the surface of the sun were oscillating in phase, the assumption that organized activity could be confined to regions of a size on the order of that of supergranules meant that one was observing on the order of 2.5×10^3 (Leighton et al., 1962) separate incoherent sources, if in fact intensity oscillations did exist.

In order to test the thesis that periodic activity at microwave frequencies is correlated with solar activity in general (Yudin, 1968 and Simon and Shimabukuro, 1971) activity indices related to the amount of solar activity present in H_α, soft solar x rays (2—12 Å), and each of several different radio frequencies were constructed for each data record. This was done in order to test for possible correlation between periodicities in the microwave spectrum and activity at different heights in the solar atmosphere. The indices were defined as follows:

$$I_{H_\alpha} = \frac{1}{T^*} \sum A_d^2$$

where

I_{H_α} = H_α activity index,

T^* = effective record length, and

A_d = apparent area of H_α flare visible on the solar surface, as given in Solar Geophysical Data.

This definition was adopted from Sawyer (1967) and is similar to the one used in Solar Geophysical Data since 1970 to classify daily H_α activity. The summation in this and the following definitions includes only flares occurring during the record period.

$$I_x = \frac{1}{T^*} \sum F_x$$

where

I_x = x-ray activity index; and

F_x = total integrated flux above background, as measured by Explorer 35 (Drake et al., 1969).

$$I_{15} = \frac{1}{T^*} \sum f_i \, t_i$$

where

I_{15} = 15,400 MHz activity index,

f_i = average integrated flux above background for 15,400 MHz flares, and

t_i = flare duration.

The data used for determining I_{15} was that taken by Sagamore Hill Radio Observatory and reported in Solar Geophysical Data.

For the sake of completeness activity indices were also defined similar to I_{15} for radio activity at 8800 MHz, 4995 MHz, and 2695 MHz, although it was realized that there is a certain degree of correlation between activity at these different frequencies. There is also no a priori reason to expect any relation between oscillatory phenomena at chromospheric heights and the higher, coronal-based radio activity.

Once the various indices were established for each data record the 40 days were divided into two groups under each type of activity index: those days having the highest index were defined as being "active" days and those with the lowest as being "quiet" days. The grouping under I_{H_α}, I_x, and for 2695 MHz had 20 days in each group. The grouping under I_{15} and for 8800 MHz and 4995 MHz had fewer days in the "active" group since flare activity was rarer for these frequencies. Consequently for these indices a record in which any kind of activity was manifested was defined as "active." Table 1 shows the list of records and to which group, by index, each was assigned.

After classifying the records into "active" and "quiet" groups under each activity index the individual power spectra in each group were averaged to obtain an "average" power spectrum. This had the effect of increasing the statistical reliability of the averaged set over that of the individual power spectra, effectively enhancing any

periodicity that might be common to all of the spectra but masked because of a low signal-to-noise ratio.

The following formula was adopted to average the spectra:

$$\bar{P}_i = \frac{1}{N} \sum_{j=1}^{N} \sigma_j^2 \exp\left(\frac{-2.3\ b}{20\sqrt{k_j - 1}}\right) P_{ij}$$

where

$\bar{P}_i$ = i'th point in the averaged power spectrum,

P_{ij} = i'th point in the j'th power spectrum,

N = number of spectra being averaged, and

σ_j = standard deviation about the mean of data in the original j'th pre-whitened data set. Since the data in the j'th data set were divided by σ_j after the mean was removed prior to calculation of the power spectrum, this weight is necessary to restore the proper relative units to P_{ij}.

k_j = degrees of freedom in j'th computed power spectrum and

b = 8 for 50% confidence limits.

The exponential weighting factor is included to properly weigh individual spectra according to its probable error. Since the weight of an experiment in an average is proportional to the reciprocal of its uncertainty this results in emphasizing the more

reliable ones. The uncertainty in individual spectra was taken to be the probable error, or the square root of the 50% confidence factor defined above.

Confidence limits for the averaged spectra were computed by assuming that its equivalent degrees of freedom equaled the sum of the degrees of freedom in the individual spectra comprising the average.

IV. RESULTS

A. Results of This Study

1. Long Data Records

The results of averaging the spectra by groups are shown in Figures 9 through 14 for the frequency range 1—15 mHz. The upper curve in each figure is the averaged spectrum for the "quiet" group under the given index, and the lower curve is for the corresponding "active" group. The two curves in each figure are normalized to the value 10 in the interval 5—6 mHz and separated by a decade for display purposes.

It is immediately apparent that there are no peaks in any of the spectra that could be considered as statistically significant compared to the 96% confidence limits. The fact that there are no outstanding peaks in either of the averaged spectra indicates that the antenna and receiving system do not introduce any periodicities in this frequency range. There does appear to be a difference in the general small-scale structure between the quiet and active curves in each case. In order to provide a more direct comparison between the spectra representing the active and quiet days, the ratio between the two spectra for a given index was taken. These results are plotted, by index, in the upper part of Figure 15 and provide a semiquantitative method of comparing the relative power in each

spectrum as a function of frequency. Error bars were assigned by adding the probable error (50% confidence) of the active and quiet spectra to yield the probable error for the ratio and then computing the 96% confidence limits from this result.

An examination of these ratios shows no significant periodicities present in the averaged active spectra that are not present in the averaged quiet spectra, though several peaks are present that appear to be marginally significant. Peaks common to H_α and x-ray activity appear at 8.0, 9.3, and 12.0 mHz and there is a general morphological similarity between the two curves. This similarity is presumably due to the fact that 13 of the records used to calculate the averages were classified as being active for both indices, thus providing a certain degree of expected correlation. A fairly well-defined peak common to the 8800 MHz and 4995 MHz indices is present at 4.3 mHz but is not considered to be statistically significant.

It may be noticed that there appears to be a general upward trend, shown by light lines in Figure 15, in the ratios for the H_α and x-ray indices. This trend would be expected if the background "continuum" of the averaged active spectrum falls off with frequency slower than that of the averaged quiet spectrum. This result indicates that turbulant activity in the chromosphere may show up as a power shift toward higher frequencies in the power spectrum, even though no discernable periodic structure appears. The absence of a similar trend in the ratios for the radio frequencies is interpreted

as meaning that little or no correlation exists between coronal-based radio activity and the existence of chromospheric-based oscillatory phenomena.

In order to test the possibility that the peaks evident in the ratios in Figure 15 were real but marginally significant, the 40 days were subdivided into two groups of 20 days each. Each subgroup of 20 was then divided into 10 "active" and 10 "quiet" days using the activity indices as guides, and the power spectra of each group averaged according to the method of the preceding section. This averaging was done for both the I_{H_α} and I_x indices; the assignment of the data sets to their respective "active" and "quiet" categories is indicated in Table 1. The ratios of averaged active to averaged quiet spectra were computed as before, providing a set of 4 curves shown in the lower-middle part of Figure 15. For each index a curve is labeled 68 or 69, that being approximately the year into which each of the 20-day groups fell.

Inspection of these curves shows that for the two indices there is no significant similarity between the structure of the 1968 averaged power spectra and that for the 1969 data. This indicates that the peaks in the original ratios calculated using all 40 days are essentially statistical in nature. It may be noticed also that the upward trend is in evidence in each of these ratio curves, especially those of H_α activity. This tends to confirm the reality of the trend.

2. Short Data Records

An investigation was also made into the effects of calculating and averaging the power spectra of many short data sets rather than those of fewer but longer data sets. This was motivated in part by the necessity of comparing the results of several authors (done in the following section), each of whom used data sets of different lengths. A more important reason stems from the fact that the data may be nonstationary in character; that is, the power spectrum of a data set of finite length changes with time. This nonstationarity would presumably result from dynamic activity in the solar atmosphere and the fact that few processes there remain constant for long periods of time.

This is particularly true of the solar oscillations. Bhattacharyya (1972) in his study of velocity oscillations at several photospheric and chromospheric heights found that the oscillations exist in the form of localized bursts in which the fluctuations rise to a maximum value and then die down. The periods between bursts and the phases of the oscillations appeared to vary randomly and there was little oscillatory motion between bursts. It was found that the mean duration of the bursts decreases with height, as does the mean fraction of time over which the oscillations exist. These findings imply that velocity data, and hence the attendant intensity data for the upper photosphere and lower chromosphere, recorded from a fixed location on the sun are highly nonstationary over short data periods.

The present experiment used a large antenna beamwidth, thus recording the fluctuations of many oscillating elements and reducing the signal-to-noise ratio to a near zero value. The nonstationarity of individual bursts would then be effectively cancelled by the superposition of many bursts. It is nevertheless instructive to test the possibility that enough nonstationarity remains such that any marginally significant periodicities are smeared out in the averaged power spectra when long data records are used. This nonstationarity would be the result of the periodicity not maintaining a constant phase or frequency over the time of each individual record.

The averaged power spectrum of several short, contiguous data records will not, in general, be the same as the power spectrum computed by considering the entire data set as a single unit. To see why this is so consider a data record $f(t)$ representing the intensity of a fixed point on the solar disc as a function of time on the interval $[T_o, T_n]$. Suppose $f(t)$ is composed of n contiguous data sets such that

$$f(t) = f_1(t) + f_2(t) + \ldots + f_n(t)$$

where $f_i(t)$ is defined on the interval $[T_{i-1}, T_i]$ and is zero elsewhere.

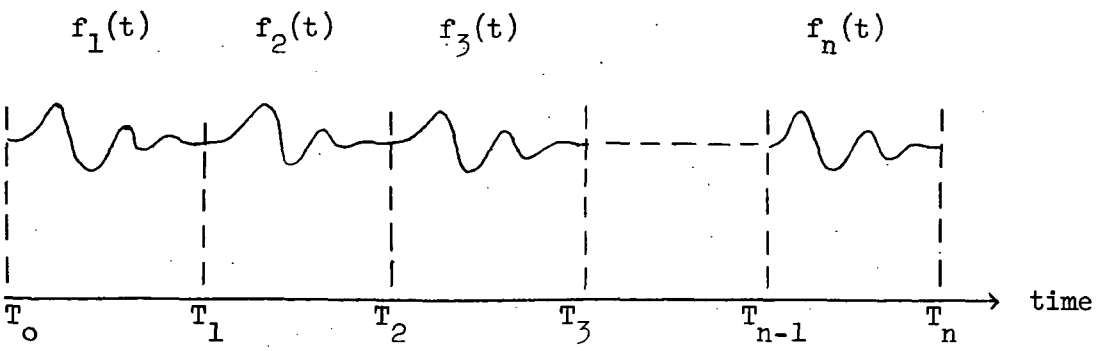

Figure 1

f(t) on the interval $[T_o, T_n]$ (see text).

The power spectrum of f(t) over the interval $[T_o, T_n]$ is then

$$P_{tot}(\omega) = \left|\tilde{f}_1(\omega) + \tilde{f}_2(\omega) + \ldots + \tilde{f}_n(\omega)\right|^2$$

$$= \left|\sum_{i=1}^{n} \tilde{f}_i(\omega)\right|^2$$

where $\tilde{f}_i(\omega)$ is the Fourier transform of $f_i(t)$.

Likewise, the averaged power spectrum composed of the average of the power spectra over the individual intervals is

$$P_{ave}(\omega) = \frac{1}{n} \sum_{i=1}^{n} \left|\tilde{f}_i(\omega)\right|^2 \quad .$$

The two results differ to the degree that the cross terms in $P_{tot}(\omega)$ fail to cancel. These cross terms appear in the power spectrum and generally express the difference between the frequency components of the average envelope modulating the individual data sets and the frequency components in the envelope modulating the entire data set. They may therefore be considered a measure of the degree of nonstationarity of the entire data set. Since we are primarily interested in the periodic structure of the individual bursts we may be better served by examining the averaged spectra of the shorter data sets; the statistical reliability will be equivalent in both cases. It is in this spirit that the following analysis was undertaken.

Although the foregoing remarks were directed toward the problem at hand, the same considerations should also apply to other problems involving power spectral analysis of nonstationary time series. It is sufficient for the present to demonstrate that the results of a power spectral analysis can be influenced by the choice of computing procedures, though a detailed analysis of the problem would involve specifying the character of the nonstationarity and assumptions regarding the ergodicity of the data set. We shall not attempt a complete analysis here. We shall instead proceed by assuming ergodicity as before and by using the knowledge of the average scale length for the bursts as reported by Bhattacharyya (1972) as a guide for determining the optimum data set length.

It was found in the above cited study that the mean burst duration for the high-forming H_β 4861 and Mg 5172 lines was 14.2 min, the H_β line being the higher of the two forming at an altitude of approximately 2200 km. This is close to the altitude at which the 2 cm radiation is observed to originate. The mean fraction of time over which the H_β oscillations were observed at a fixed location was 0.19, yielding a mean burst period of ~ 75 min.

Since the mean burst duration is given for the H_β and Mg lines considered together, and since the mean burst duration was demonstrated to decrease markedly with height, we may assume that for the H_β considered separately the duration is less than the figure cited. If a mean burst duration of 10 min is adopted for the H_β oscillations the mean burst period becomes ~ 50 min.

In the present study the 40 data sets were accordingly each subdivided into 50 min data sets. The power spectrum was computed for each of these 50 min periods using the Blackman-Tukey method with a maximum lag of 25 min as before. Although the statistical reliability of the power spectral estimates for each 50 min data set was much reduced over that of the day taken as a whole, the confidence limits of the averaged 50 min power spectra were equivalent to those of the latter. Using the activity indices constructed for H_α activity as a guide, all of the 50 min spectra belonging to the "active" group were averaged using the previously defined averaging formula. The same was done for the "quiet" data, and the ratio of the resultant averaged spectra taken as before.

The ratio, labeled "short records", is displayed in the bottom of Figure 15. It is apparent that there is no statistically significant periodicity evident, thus confirming the results of the study using the full data sets. The upward trend is again in evidence, although not to as marked a degree as in the previous experiments using the H_α indices. The detailed structure is similar to that of the H_α ratio, confirming that the data taken as a whole is nearly stationary and that little or no periodic activity is present.

We thus conclude that for the 40 days of data used in this study there is no evidence of statistically significant periodic activity. Such activity may indeed exist but its amplitude must either be below the level of detection or it could consist of periodicities with a dispersion in periods sufficiently wide to smear out any discernable peaks. We also conclude that because of the absence of detectable constant periodic activity in this experiment there is no apparent correlation between solar activity and the oscillatory phenomena. The increased activity may nevertheless be manifested by the shift of power from low to high frequencies as indicated by the slight upward trend in the ratio curves.

B. Comparison With the Results of Similar Studies

The lack of detection of any periodic activity in this experiment was unexpected in light of similar studies made of the oscillatory phenomenon at microwave frequencies. In particular those studies by Yudin (1968), Durasova et al. (1971), and Simon and Shimabukuro

(1971) all reported having detected intensity fluctuations in solar microwave radiation. Their results, however, did not all agree with one another in the detected period. It is therefore worth reviewing their respective results with a view toward establishing the statistical reliability of the peaks in their power spectra and comparing, from a common base, those results with those of the present study.

1. Yudin (1968)—Fluctuations at 3.3 cm

This was the first reported observation of intensity modulation of solar microwave radiation obtained from data taken on an instrument with an angular resolution of 24 arc min. It was found that when active regions appeared on the sun radiometer output fluctuations increased markedly, with a frequency of repeatability of 70—80% over a period of 3 1/2 years.

A power spectrum analysis was performed on data corresponding to the appearance of active regions on the sun and the results compared with power spectra obtained from data from the quiet sun. No mention is made in the paper of how an active region is defined, but is taken to mean a localized enhancement of activity as evidenced by H_α spectroheliograms or the appearance of plages, flares, or other phenomena commonly associated with solar activity. The power spectrum of an active period typically showed a large peak near 300 sec with an intensity of 2—4 times that of the quiet sun (see Figure 16).

Although it is not explicitly stated how the power spectrum was computed the absence of a large low-frequency (zero) peak implies

that the data is nearly all random noise, except for that part appearing in the peak at ~ 300 sec. This is incompatable with the assumption that intensity fluctuations result from turbulence in the upper photosphere and lower chromosphere. The power spectrum of turbulence-induced oscillations should have a large low-frequency component (Noyes, 1967), and since the large antenna beamwidth assures coverage of nearly the entire disc of the sun, including non-active areas, such a component is expected. This would be in agreement with what was found by Simon and Shimabukuro (1971) and the present study. The absence of this low-frequency power suggests, therefore, some kind of data pre-processing, perhaps similar to that done by Durasova et al. (1971; see section 2 below) that would alter the true shape of the spectrum.

Although no mention was made of how the confidence limits in the computed spectra were estimated one can readily calculate them from the information given in the paper. In this and the following sections it is assumed that confidence limits as calculated from Blackman and Tukey (1958) are the true measure of statistical reality.

An estimate for the equivalent degrees of freedom can be made from a knowledge of the frequency resolution of the power spectrum and the length of the data set, or quantities derivable from these two. This is true regardless of the actual method of calculating the power spectrum (mean-lagged-product or fast-Fourier-transform) since frequency resolution and maximum frequency are set by the

uncertainty principle. We can therefore treat a power spectrum as if it were computed using the mean-lagged-product method to derive estimates of the statistical parameters necessary for determining the confidence limits.

Figure 16 taken from the cited paper shows three power spectra of data taken from the active sun, each with a broad peak near 300 sec. The lengths of the data sets from which the spectra were computed are given as 120 min, 70 min, and 58 min, respectively. The frequency resolution appears to be $\Delta f \approx 0.5$ mHz, from which the equivalent maximum lag M of the autocorrelation function would be 1000 sec. Using the formula for equivalent degrees of freedom given in the previous section we calculate k as being 13.7, 7.8, and 6.3 for the three spectra. This corresponds to 96% confidence factors of 5.0, 9.2, and 12.4, respectively. These factors provide wide margins within which the respective peaks should fall in order to be statistically significant. The reported peaks all appear to be significant, therefore, although only marginally so.

2. Durasova et al. (1971)—Fluctuations at 3.3 cm

A second measurement was made at the same frequency and by using one of the same instruments as Yudin (1968) but adding a second instrument for cross-correlation studies to help eliminate tropospheric influences. The effective beamwidths of the 2-antenna combination was 33 arc min, thus covering the entire disc of the sun.

The method of examining the data for periodic structure is given as being similar to that used by Yudin. We note that again there is no low-frequency peak in any of the spectra presented, which may be due to the stationarization by "... continuous summation ..." referred to in the paper. As in the previous case, it is unknown how much this procedure would alter the appearance of the spectrum. There was no attempt by the authors to place confidence limits on the resultant spectra.

The cited paper gives the maximum lag of the autocorrelation function as being ~ 47 min, from whence the frequency resolution $\Delta f \sim 0.17$ mHz. An examination of the small-scale structure of Figure 17 indicates that this must be approximately correct though the spectra are drawn as being continuous. The three curves of Figure 17 are reported to have been calculated from data sets respectively 180 min, 178 min, and 159 min long, for which the equivalent degrees of freedom are calculated to be 7.0, 6.9, and 6.1. These figures translate into 96% confidence factors of 4.6, 4.6, and 5.0, respectively, making the individual peaks in the spectra appear to be only marginally significant. Figure 18, however, shows the average of 22 power spectra with two well-defined peaks at 280 and 400 sec, and a broad peak at ~ 900 sec. If we assume a figure of 7 for the equivalent degrees of freedom for each individual power spectrum used in making the average we arrive at a 96% confidence factor of 1.6. The peaks thus appear to be significant.

3. Simon and Shimabukuro (1971)—Fluctuations at 3.3 and 3.5 mm

The last of the three reports of periodic activity at microwave frequencies was made by analyzing data taken on the NRAO Kitt Peak 36 ft radiotelescope with a beamwidth of 1.2 arc min at a wavelength of 3.5 mm and on the Aerospace Corporation 15 ft radiotelescope with a beamwidth of 2.8 arc min at a wavelength of 3.3 mm. The power spectra were computed using the Blackman-Tukey algorithm for the Kitt Peak data and the fast-Fourier-transform method on the Aerospace data. No confidence limits were placed on the presented spectra by the authors.

One can compute the expected confidence for the various figures shown from data supplied in the body of the paper. Thus Figure 19 shows the power spectrum of a single data set of length 50 min taken with 1.42 sec data sample spacing for a total of 2160 samples. Δf is specified as being ~ 0.30 mHz, from which we calculate the equivalent maximum lag of the autocorrelation function as being $M \sim 1670$ sec. This is more than half the length of the data set so we must conclude that M is actually 1500 sec, setting $\Delta f = 0.33$ mHz. The equivalent degrees of freedom for this power spectrum are then ~ 2.7, making even the 50% confidence factor on the order of 2. Thus the peaks shown at 3.5 and 5.6 mHz are definitely of questionable reality.

Figure 20 shows the averaged power spectra observed over undisturbed regions for both the 3.3 and 3.5 mm data. Our analysis of the parameters relating sampling time and data record lengths provided 96% confidence factors of 2.2 and 2.6, respectively, for these wavelengths. The 96% confidence factors for the averaged power spectra observed over disturbed regions (Figure 21) were calculated to be 1.5 and 3.0. It therefore appears that one may safely doubt the reality of the observed peaks in the averaged power spectra as well as in the individual case shown in Figure 19.

The main results of the three previous papers that are of interest to this study are summarized below along with an assessment, based on the foregoing analysis, of the reality of the principal peaks in the reported power spectra.

Investigator	Period (sec)	Frequency (mHz)	Assessed Reality of Results
Yudin (1968)	275	3.6	marginal
Durasova et al. (1971)	400 280	2.5 3.6	apparently real
Simon and Shimabukuro (1971)	180	5.6	doubtful
Present work	none	--	real

It is difficult to reconcile the results of these studies and the present one with one another. The small beamwidths of the instruments used by Simon and Shimabukuro should have resulted in a decidedly better signal-to-noise ratio with respect to the intensity modulations than the large beamwidths used in the other studies. If

the oscillations exist as coherent intensity fluctuations on a size the order of that of a supergranule the 3 mm instruments would be looking at ~ 5—10 separate oscillating sources, whereas for the centimetric data ~ 2.5×10^3 sources would be visible. Additionally the millimetric study would be looking at fluctuations at a lower altitude than the centimetric studies. Hence, if one assumes that the relative amplitudes of the oscillations decrease with height, one would expect the 3 mm study to show a peak in the power spectrum if amplitude fluctuations were present. It is not immediately clear why large peaks therefore appear in the 3.3 cm studies but none in the millimetric spectra. The same might also be said concerning the lack of any detectable period in the present 2 cm study versus the large peaks in the two 3.3 cm reports; all three experiments were made at comparable wavelengths and all used instruments of large antenna beamwidth.

V. A MODEL FOR OSCILIATION BURSTS

The recent work of Bhattacharyya (1972) referred to in the previous section suggests a model for the morphology of the oscillations at chromospheric heights. This model may be used as a starting point for estimating several useful parameters that may be helpful in future planning for the detection of these oscillations. In the following sections the model is given and estimates of the minimum signal-to-noise ratio for which a signal can be confidently detected are derived. Estimates for an upper limit to the ratio of the mean peak-to-peak to ambient temperature for the oscillations at chromospheric heights above a supergranule are made. An upper limit for the mean fraction of the quiescent solar surface experiencing oscillations at any given time is also estimated, and an expression for the minimum amount of data needed for detection of the periodicities at microwave frequencies is given.

A. The Model

As mentioned in section IV, Bhattacharyya found the oscillations to exist as localized bursts with well-defined times for mean burst duration and mean burst period. At heights characteristic of H_β line formation the bursts were found to have a mean duration of 14.2 min, and we set a value of ~ 50 min for the mean burst period. Although the physical area over which the oscillations remain

coherent at chromospheric heights is unknown, the work of Bhatnagar and Tanaka (1972) suggests that the fluctuations may be coherent over an area approaching that of a supergranule.

Figure 22 shows how these bursts would appear if they are exponentially damped with a 1/e damping time of 15 min. Although the period of the oscillations is shown as being 5 min, it may in fact be shorter. The actual period is unimportant in the following analysis as long as it is short compared to the damping time. Additionally, there may be noise superimposed on the bursts.

B. Derivation of the Minimum Signal-to-Noise Ratio for Which A Monochromatic Signal Can Be Confidently Detected

In order to determine the detectability of a signal imbedded in noise we begin by considering the case of a monochromatic sinusoid of constant amplitude A impressed on stationary noise approximated by Gaussian noise of standard deviation σ. Let

B_n = noise power per elementary frequency interval Δf,

B_s = signal power per elementary frequency interval Δf, and

S = signal-to-noise ratio.

Then

$$S = \frac{A^2}{2}\frac{1}{\sigma^2} = \frac{B_s}{B_n m} \tag{1}$$

where m is the number of elementary frequency intervals Δf in the power spectrum containing the full power. Now

$$m\Delta f = \frac{1}{2\tau_s}$$

where τ_s is the data sample period in seconds, so that

$$S = 2\tau_s \, \Delta f \, \frac{B_s}{B_n}$$

or

$$\frac{B_s}{B_n} = \frac{S}{2\tau_s \, \Delta f} \quad .$$

Let

f_c = 96% confidence multiplicative factor

$$= \sqrt{(96\% \text{ confidence factor})}$$

$$= \exp\left(\frac{2.88}{\sqrt{k - 1}}\right)$$

where k is equal to the degrees of freedom. For 96% confidence signal detection we must therefore have

$$\frac{B_n + B_s}{B_n} = 1 + \frac{B_s}{B_n} \geq f_c$$

from which

$$S \geq 2\tau_s \, \Delta f \, (f_c - 1) \quad .$$

Let S_n denote the minimum signal-to-noise ratio for detection with 96% confidence. Then

$$S_n = 2\tau_s \, \Delta f \left[\exp\left(\frac{2.88}{\sqrt{k - 1}} \right) - 1 \right] \quad . \tag{2}$$

Now

$$k = 2 \left(\frac{N}{m} - \frac{1}{3} \right)$$

$$\approx 2 \frac{N}{m} \quad \text{for large amounts of data } (N \gg m),$$

where

N = total number of data points in data records and

m = equivalent maximum number of lags in the autocorrelation function

= the number of elementary frequency intervals in the power spectrum.

Therefore

$$k \approx 2 \frac{N\tau_s}{m\tau_s} = \frac{2T}{\frac{1}{2\tau_s \Delta f}\ \tau_s}$$

$$= 4T\Delta f \qquad (3)$$

where $T = N\tau_s$, the total amount of data in seconds. Substituting Eq. (3) into (2) and assuming $k \gg 1$, we obtain

$$S_n \approx 2\tau_s \Delta f \left[\exp\left(\frac{1.44}{\sqrt{T\Delta f}}\right) - 1\right] \quad .$$

In the above expression for S_n and in the following sections 96% confidence is used to define detectability. Figure 23 shows S_n as a function of k for several different confidences with m = 50. Figure 24 shows the results of one of several tests where signals of several different amplitudes were impressed on random noise with an added trend. These tests confirmed the results of the derivation of S_n.

C. Application to the Model to Calculate the Burst Amplitude for the Quiescent Sun

From Eq. (1) the minimum detectable amplitude A_{min} of a monochromatic signal is

$$A_{min} = \sigma\sqrt{2S_n} \quad .$$

σ is the rms noise as viewed in the digitized data about the instantaneous mean in a given data set. As such it depends upon the integration time for each data sample. If σ_o is taken as the standard rms noise for a data sample integration time τ_i of 1 sec, we have

$$\sigma = \frac{\sigma_o}{\sqrt{\tau_i}} \quad .$$

Hence

$$A_{min} = \sigma_o \sqrt{\frac{2S_n}{\tau_i}} \quad .$$

It is desired to calculate the minimum detectable $\Delta I/I$ (the ratio of burst peak-to-peak to ambient temperature as measured at the receiver output) for a single burst exponentially damped as shown in Figure 22.

We define

$$g = \frac{\text{(power in a monochromatic signal)}}{\text{(power in a single damped burst wave train)}}$$

$$\approx \frac{1}{\frac{1}{t_b}\int_o^{t_b} [h(t)]^2 \, dt}$$

where

t_b = burst period,

h_t = waveform modulating the burst

$= e^{-t/\tau_b}$ for exponential damping, and

τ_b = mean burst duration.

If ΔI_{min} is equal to the minimum detectable peak-to-peak burst amplitude,

$$\Delta I_{min} = 2A_{min}\, g = 2\sigma_o\, g\sqrt{\frac{2\mathcal{E}_n}{\tau_i}}$$

where it is assumed that the spreading Δf_ℓ of the peak in the power spectrum due to short burst duration is such that $\Delta f_\ell < \Delta f$. For the present model $\Delta f_\ell \approx 0.16$ mHz so this criterion is satisfied.

When the sun is in the quiescent state the visible surface contains $\sim 2.5 \times 10^3$ supergranules. If each is considered to be an

independent source of coherent oscillations of random phase and mean peak-to-peak amplitude ΔI and if N_s denotes the number of sources viewed simultaneously in the radiotelescope beam,

$$\frac{\Delta I_{min}}{I_o} \approx \frac{2A_{min}\, g\sqrt{N_s}}{I_o} = \frac{2\sigma_o\, g}{I_o}\sqrt{\frac{2N_s\, S_n}{\tau_i}}$$

where $\Delta I_{min}/I_o$ is the minimum detectable ratio of temperature fluctuation peak-to-peak amplitude to mean ambient temperature I_o. Thus

$$\frac{\Delta I_{min}}{I_o} \approx \frac{4\,\sigma_o\, g}{I_o}\sqrt{N_s\,\frac{\tau_s}{\tau_i}\;\Delta f\left[\exp\left(\frac{1.44}{\sqrt{T\Delta f}}\right) - 1\right]} \quad . \tag{4}$$

This equation assumes that the frequency dispersion of the bursts over N_s sources is smaller than Δf.

One can evaluate these relations for the parameters of the present study to calculate $\Delta I_{min}/I_o$. For the total "quiet" data

$$N_s \approx 2.5 \times 10^3,$$

$$\tau_s = 30 \text{ sec},$$

$$\sigma_o/\sqrt{\tau_i} = \sigma$$

$$= 10 \text{ K},$$

$I_o \approx 10^3$ K,

$T \approx 140$ h

$\approx 5 \times 10^5$ sec,

$\Delta f = 0.33 \times 10^{-3}$ Hz, and

$g = 6.67$ for the present model.

Putting these figures into Eq. (4) results in a value of $(\Delta I_{min}/I_o) \approx 0.46$. The large magnitude of this figure helps to understand why no periodicity was observed in the averaged quiet spectra, for no evidence exists that oscillations of such a large amplitude exist uniformly scattered over the solar surface.

The same procedure may also be carried out for the best case for the quiet data of Simon and Shimabukuro. Thus

$N_s \approx 10$ for a beamwidth of ~ 2.8 arc min,

$\tau_s = 6$ sec,

$\sigma_o/\sqrt{\tau_i} = 6$ K,

$I_o \approx 10^4$ K,

$\Delta f = 0.33 \times 10^{-3}$ Hz,

$T \approx 5.5 \times 10^4$ sec, and

$g = 6.67$.

These figures yield $(\Delta I_{min}/I_o) \approx 1.5 \times 10^{-3}$.

The fact that no periodicities were observed over quiet regions indicates that this figure must approximately equal the upper limit for the mean $\Delta I/I$ for a supergranule. The $\Delta I/I$ of a localized area within the supergranule may of course be larger than this upper limit if the oscillatory motion is not spread uniformly over the supergranule but is instead confined to small regions. Such a possibility is suggested by the recent work of Tanaka (1973) where it was found that in H_α plages oscillating elements occupy between 2 and 9% of the total plage area at any given instant. The remaining area showed little or no periodic motion.

Although the difference between the physical conditions of the chromosphere in quiescent regions of the sun and those in plages are such that one could not immediately assume that oscillations in quiescent supergranules are similarly limited in size, it may be that this is actually the case. High resolution $\Delta I/I$ measurements are not available for chromospheric oscillations, but investigations into the phenomenon as measured in the CO vibration-rotation line at 4.67μ by Noyes and Hall (1972) give a $\Delta I/I$ of 7% for the high photosphere. If this figure is assumed to hold for the higher millimetric emission heights observed by Simon and Shimabukuro (1971) and the upper limit of 1.5×10^{-3} as previously calculated is taken to be the approximate

mean $\Delta I/I$ for a supergranule in a quiescent state, an upper limit of ~ 0.02 for the mean ratio of oscillating area to total supergranule area is indicated. This upper limit is in reasonable agreement with the figure obtained by Tanaka (1973) for plage-based oscillations in H_α.

D. Other Useful Parameters

From the previous section it is apparent that in order to study the oscillatory motions of the quiescent chromosphere at radio frequencies small antenna beamwidths are necessary if the total amount of data needed for detection is to be kept reasonably small. It is possible to make estimates of the minimum detectable $\Delta I/I$, minimum beamwidth, or the minimum amount of data required for detection as functions of relevant instrument parameters.

For example, if it is assumed that antenna beamwidths will be kept smaller than ~ 20 arc min,

$$N_s \approx 2.5 \times 10^3 \times \frac{1}{2} \left(\frac{BW'}{32'}\right)^2$$

where

BW' = antenna beamwidth, arc min; and

$32'$ = solar diameter.

One also recognizes that the oscillations are not, in general, monochromatic but show an associated dispersion in frequency. Suppose

the oscillations are slightly but uniformly dispersed in frequency with a dispersion width equal to $p\Delta f$, where $p > 1$. Then from Eq. (1)

$$S = \frac{B_s}{B_n\ p\ m}$$

so that

$$S_n = 2\tau_s\ p\Delta f\ (f_c - 1) \quad .$$

Let R_I denote the minimum detectable mean peak-to-peak source amplitude if the beamwidth and dispersion are known. Then from Eqs. (2) and (4)

$$R_I \approx \frac{4.4\ \sigma_o\ gBW'}{I_o} \sqrt{\frac{\tau_s}{\tau_i}\ p\Delta f\ \left[\exp\left(\frac{1.44}{\sqrt{T\Delta f}}\right) - 1\right]} \quad .$$

One may invert this to solve for the minimum beamwidth needed to detect a given R_I:

$$BW' \approx \frac{0.23\ R_I\ I_o}{\sigma_o\ g} \left\{\frac{\tau_s}{\tau_i}\ p\Delta f\ \left[\exp\left(\frac{1.44}{\sqrt{T\Delta f}}\right) - 1\right]\right\}^{-1/2} \quad .$$

If it is desired to determine the minimum amount of data time $T_<$ required to confidently detect the periodicity, we solve

$$T_< \approx \frac{2}{\Delta f} \left\{ \log \left[1 + \frac{1}{p \Delta f} \frac{\tau_i}{\tau_s} \left(\frac{0.23 \, R_I \, I_o}{\sigma_o \, g BW'} \right)^2 \right] \right\}^{-2} \quad . \qquad (5)$$

An example of how Eq. (5) might be useful is to consider an ideal experiment and estimate the minimum amount of data required to detect the oscillations. Suppose an experiment using the NRAO Kitt Peak 36 ft instrument at a wavelength of 1 mm is considered. We assume equipment and data parameters that might reasonably be expected to be the following:

aperture efficiency $\approx 20\%$

$\Delta f = 0.33 \times 10^{-3}$ Hz ,

$\tau_s = 30$ sec,

$p = 2$,

$BW' = 0.7$ arc min,

$g = 6.67$,

$\sigma_o / \sqrt{\tau_i} = 5$ K,

$R_I = 1.5 \times 10^{-3}$, and

$I_o = 10^4$ K.

The Δf and τ_s are chosen to allow for reasonable frequency resolution and maximum statistical reliability in the frequency range 0—16.7 mHz. A frequency dispersion of $2\Delta f$ is allowed and g is calculated from the present model. R_I is assumed to be approximately the same as the minimum detectable $\Delta I/I$ calculated above for Simon and Shimabukuro.

Substitution of these figures into Eq. (5) yields

$$T_< \approx 4.5 \times 10^3 \text{ sec} = 1.25 \text{ h} \quad .$$

Thus only a few hours of data would be needed in this experiment to achieve a statistical reliability equaling that of Simon and Shimabukuro. We note also that with the given small beamwidth the number of sources N_s that would be viewed is $\sim$ 1—2. It should therefore be possible to accurately determine g and either R_I or the mean fraction of the source surface area experiencing oscillations at any time by examining more than the minimum required amount of data.

In this chapter several useful expressions were developed using the statistical properties of power spectra. These expressions were applied to a model of the oscillation bursts for the quiescent sun to yield estimates for oscillation amplitude and the mean fraction of area experiencing oscillations. One could extend the analysis to consider active areas of the solar surface. The assumptions

required to do so would include the coherence length of the oscillations and the character of the oscillation bursts. Since neither of these quantities are well established for active regions at chromospheric heights, the present work does not consider them.

VI. CONCLUSIONS

The conclusions of this thesis are as follows:

(1) A power spectral analysis of 285 h of 2 cm microwave intensity data showed no statistically significant (> 96% confidence) periodicities in the frequency range 1—15 mHz. No correlation was found between 2 cm periodicities and solar activity in H_α, x-ray, and several microwave frequencies.

(2) A small shift of power toward higher frequencies in the power spectrum of the 2 cm data was found to be correlated with solar H_α and x-ray activity. This power shift is attributed to increased chromospheric turbulence due to solar activity at altitudes common to H_α, x-ray and 2 cm emission.

(3) A consistent statistical analysis of previous works reporting evidence for the oscillations at microwave frequencies indicates that confidence in these previous results is marginal.

(4) Using the statistical properties of power spectra, an expression for the ratio of the minimum detectable peak-to-peak to ambient temperature at chromospheric heights may be derived. Applied to a model for oscillation bursts in quiescent supergranules and using the most significant results to date of experiments to detect the microwave periodicities, this expression yields an upper limit of $\sim 1.5 \times 10^{-3}$.

(5) Based on the most significant results of microwave periodicity experiments, the mean ratio of oscillating area to total quiescent supergranule area at chromospheric heights is calculated to have an upper limit of ~ 0.02. This upper limit is in reasonable agreement with the results of previous direct measurements made of oscillating elements in H_α plages.

(6) The minimum amount of solar microwave data required for detection of the periodicities may be estimated as a function of equipment and data parameters. Assuming reasonable parameters, the minimum required amount of data for an ideal experiment utilizing the NRAO Kitt Peak 36 ft radiotelescope at a wavelength of 1 mm is calculated to be ~ 1.25 h.

Table 1

X—Active days in full study. (X)—Active days in cross-68/69 study using H_α and x-ray indices.

Year	Day	Mins. Data	H_α		X ray		15,400	8800	4995	2695
1969	251	540	X	(X)	X	(X)	X	X	X	X
	252	270	X	(X)	X	(X)				
	255	270	X	(X)	X	(X)				X
	256	510		(X)		(X)				X
	258	420				(X)				X
	259	360								
	260	240								
	266	420	X	(X)						
	269	500	X	(X)	X	(X)		X	X	X
	271	480	X	(X)		(X)		X	X	X
	273	360			X	(X)				
	274	460						X	X	
	277	240								
	278	480	X	(X)	X	(X)				X
	281	520		(X)						X
	328	390	X	(X)			X	X	X	X
	337	360			X	(X)				
	341	300								
	342	240						X	X	
	343	300								X
	344	420	$\bar{X}$	$\bar{(X)}$	$\bar{X}$	$\bar{(X)}$	X	X	X	X
	349	390			X	(X)				
1969	40	250	X	(X)	X					
	121	500								
	132	600	X	(X)	X	(X)				X
	134	480	X	(X)						X
	136	460	X					X	X	
	139	510	X	(X)	X	(X)		X	X	X
	142	380	X	(X)					X	X
	144	360	X	(X)			X	X	X	X
	148	420	X	(X)	X		X	X	X	X
	150	420			X	(X)		X	X	
	152	540			X	(X)				
	154	710	X		X	(X)				X
	178	630			X					
	185	510								
	191	600			X	(X)				
	193	540	X	(X)	X	(X)			X	X
	195	360	X	(X)	X	(X)	X	X	X	X
	211	400								

ACKNOWLEDGMENTS

The author would like to express his sincere appreciation and gratitude to Dr. Stanley Shawhan for proposing this project, which was originally considered in an undergraduate reading research assignment. His advice and direction were indispensable for bringing the research to a satisfactory conclusion.

Dr. James Van Allen is thanked for providing support during the several years the author was a graduate student in the department, and for making available the Explorer 35 x-ray data used in part of this work.

Dr. John Fix is thanked for helping to clarify several points related to the understanding of the theory.

I should like to thank Dr. Charles Wende for providing the large body of solar microwave data taken while he was at the University of Iowa.

Much of the tedious work done in the digitization of the data was done by Mr. Gerald Denning. His assistance is greatly appreciated.

Mr. Steven Spangler, with whom I have shared an office, deserves an expression of thanks for his many helpful discussions on the topic.

Thanks are due to Miss Shirley Streeby who completed the typed copy of this thesis despite what must have seemed like deliberate attempts by the author to create extra work for her. Mr. John Birkbeck

and the drafting staff are thanked for drawing the excellent plots used in this work.

Finally, I should like to acknowledge the helpful assistance of the Data Analysis staff and their willingness to accomodate unusual user requests.

Support for this thesis has been provided by the Office of Naval Research through contract N00014-68-A-0196-0003 and the National Aeronautics and Space Administration through grant NGL-16-001-002.

LIST OF REFERENCES

Bhatnagar, A. and Tanaka, K.: 1972, 'Intensity Oscillation in H_α-Fine Structure', Solar Phys. 24, 87.

Bhattacharyya, J. C.: 1972, 'Velocity Oscillations in the Solar Atmosphere', Solar Phys. 24, 274.

Blackman, R. B. and Tukey, J. W.: 1958, The Measurement of Power Spectra (New York, Dover Publications).

Collins Radio Company: 1967, 'Theory of Operation, 2-cm Radiometer—Polarimeter', Univ. of Iowa Dept. of Phys. and Astronomy Publication.

Drake, J. F., Van Allen, J. A., and Gibson, J.: 1969, 'Iowa Catalog of Solar Soft X-Ray Flux (2—12 Å)', Solar Phys. 10, 433.

Durasova, M. S., Dobrin, M. M., and Yudin, O. I.: 1971, 'Evidence of Quasi-Periodic Movements in the Solar Chromosphere and Corona', Nature 229, 82.

Edmonds, F. N., Jr.: 1966, 'A Coherence Analysis of Fraunhofer-Line Fine Structure and Continuum Brightness Fluctuations Near the Center of the Solar Disc. II', Astrophys. J. 144, 733.

Elliott, I.: 1969, 'Power Spectra of H_α Doppler Shifts', Solar Phys. 6, 28.

Evans, J. W. and Mitchard, R.: 1962, 'Observational Study of Macroscopic Inhomogeneities in the Solar Atmosphere. III. Vertical Oscillatory Motions in the Solar Photosphere', Astrophys. J. 136, 493.

Gotwols, B. L.: 1971, 'Quasi-Periodic Solar Radio Pulsations at Decimetric Wavelengths', Johns Hopkins Univ. Applied Physics Lab. Preprint.

Holloway, J. L., Jr.: 1958, 'Smoothing and Filtering of Time Series and Space Fields', Advances in Geophysics 4, 351.

Howard, R.: 1962, 'Preliminary Solar Magnetograph Observations With Small Aperatures', Astrophys. J. 136, 211.

Kaufmann, P.: 1972, 'Possible Long-Period Oscillations in Solar Radio Emission at Microwaves', Solar Phys. 23, 178.

Kobrin, M. M. and Korshunov, A. I.: 1972, 'On Quasi-Periodic Components with Periods From 30 to 60 min of Amplitude Fluctuations of X-Band Solar Radio Emission', Solar Phys. 25, 339.

Krauss, J. D.: 1966, Radioastronomy (New York, McGraw-Hill).

Leighton, R. B., Noyes, R. W., and Simon, G. W.: 1962, 'Velocity Fields in the Solar Atmosphere. I. Preliminary Report', Astrophys. J. 135, 474.

Noyes, R. W.: 1967, 'Observational Studies of Velocity Fields in the Solar Photosphere and Chromosphere' in R. N. Thomas (ed.), 'Aerodynamic Phenomena in Stellar Atmospheres', IAU Symp. 28 (New York, Academic Press).

Noyes, R. W. and Hall, D. N. B.: 1972, 'Thermal Oscillations in the High Solar Photosphere', Astrophys. J. 176, 289.

Noyes, R. W. and Leighton, R. W.: 1963, 'Velocity Fields in the Solar Atmosphere. II. The Oscillatory Field, Astrophys. J. 138, 631.

Sawyer, C. B.: 1967, 'A Daily Index of Solar Flare Activity', J. Geophys. Res. 72, 385.

Simon, M. and Shimabukuro, F. I.: 1971, 'Observations of the Solar Oscillatory Component at a Wavelength of 3 mm', Astrophys. J. 168, 525.

Tanaka, K.: 1973, 'Chromospheric Oscillation in H_α', California Inst. of Technology, Big Bear Observatory Preprint.

Wende, C. D.: 1968, 'The Correlation of Solar Microwave and Soft X-Ray Radiation', Univ. of Iowa Dept. of Phys. and Astronomy, Ph.D. Thesis.

Wende, C. D.: 1969, 'The Handbook of the NLRO 2-cm Solar Patrol' (1st Ed.), Univ. of Iowa Dept. of Phys. and Astronomy Publication.

Whitney, C.: 1958, 'Granulation and Oscillations of the Solar Atmosphere', Smithsonian Contrib. Astrophys. 2, 365.

Yudin, O. I.: 1968, 'Quasiperiodic Low-Frequency Solar Radiowave Fluctuations', Soviet Phys.—Dokl. 13, 503.

LIST OF FIGURES

Figure 9 Averaged power spectra for quiet and active days as defined using the H_α activity indices described in the text.

Figure 10 Averaged power spectra using x-ray activity indices.

Figure 11 Averaged power spectra using 15,400 MHz activity indices.

Figure 12 Averaged power spectra using 8800 MHz activity indices.

Figure 13 Averaged power spectra using 4995 MHz activity indices.

Figure 14 Averaged power spectra using 2695 MHz activity indices.

Figure 15 Ratios of averaged active to averaged quiet power spectra. The top six curves show the ratios, by index, of the curves in Figures 9 through 14. The two sets of curves labeled "H_α" and "x-ray" each have curves labeled "68" and "69". Each of these latter curves represents the ratio of the averaged power spectra of 10 active to that of 10 quiet days. The bottom curve is the ratio of active to quiet (as defined by H_α activity indices) power spectra computed from the short (50 min) records into which the long data sets were divided.

Figure 16 Power spectra of three daya segments given as evidence for the existence of the 300 sec periodicities by Yudin (1968). The 96% confidence limits, computed on the basis of the analysis presented in the text, were added to Yudin's original figure. The lengths of the respective data sets are given as 120 min (cross), 70 min (circle), and 58 min (square) from which the confidence limits were computed. (After Yudin, 1968.)

Figure 17 The three power spectra reported by Durasova et al. (1971) that show detailed structure. The frequency resolution is calculated to be 0.17 mHz and the 96% confidence limits were added to the original figure. (After Durasova et al., 1971.)

Figure 18 The average of 22 power spectra similar to the three shown in Figure 17. The confidence limits were added to the original figure. (After Durasova et al., 1971.)

Figure 19 Sample power spectrum as given in Simon and Shimabukuro (1971) for a single data set of 50 min length. The 50% confidence limits for the degrees of freedom $k \sim 2.7$ indicate that the spectral estimates for this single data set should be considered unreliable. (After Simon and Shimabukuro, 1971.)

Figure 20 Averaged power spectra observed over undisturbed regions by Simon and Shimabukuro (1971). The 3.5 mm curve is the average of the power spectra of 9 records, while the 3.3 mm curve is the average for 13 records. The confidence limits were added to the original figure. (After Simon and Shimabukuro, 1971.)

Figure 21 Averaged power spectra for disturbed regions. The 3.5 mm curve is the average of the power spectra of 7 records, while the 3.3 mm curve is the average for 39 records. The confidence limits were added to the original figure. (After Simon and Shimabukuro, 1971.)

Figure 22 The model for oscillation bursts suggested by the work of Bhattacharyya (1972). The figure shows how the brightness I of a localized oscillating source would appear if the bursts occur as exponentially damped wave trains of random phase with mean burst duration (damping time) of 15 min and mean burst period of 50 min.

Figure 23 The minimum signal-to-noise ratio required for detection of a monochromatic sinusoid as a function of degrees of freedom k for several confidences. The maximum number of lags m in the associated autocorrelation function used to calculate these curves was 50, the same number that was used to calculate the power spectra in this study.

Figure 24 Results of one of a series of computer tests performed to verify the equation for minimum signal-to-noise ratio S_n. A signal of amplitude A was added to computer-generated Gaussian noise with standard deviation σ. A small parabolic trend was also added to the data to produce a low-frequency peak in the power spectrum similar to the peak observed in the actual power spectra of the 2 cm data. The power spectrum was then calculated for each of several different signal amplitudes. It can be seen that as the signal-to-noise ratio S approaches S_n the peak corresponding to the signal becomes lost in the statistical "noise" of the power spectrum.

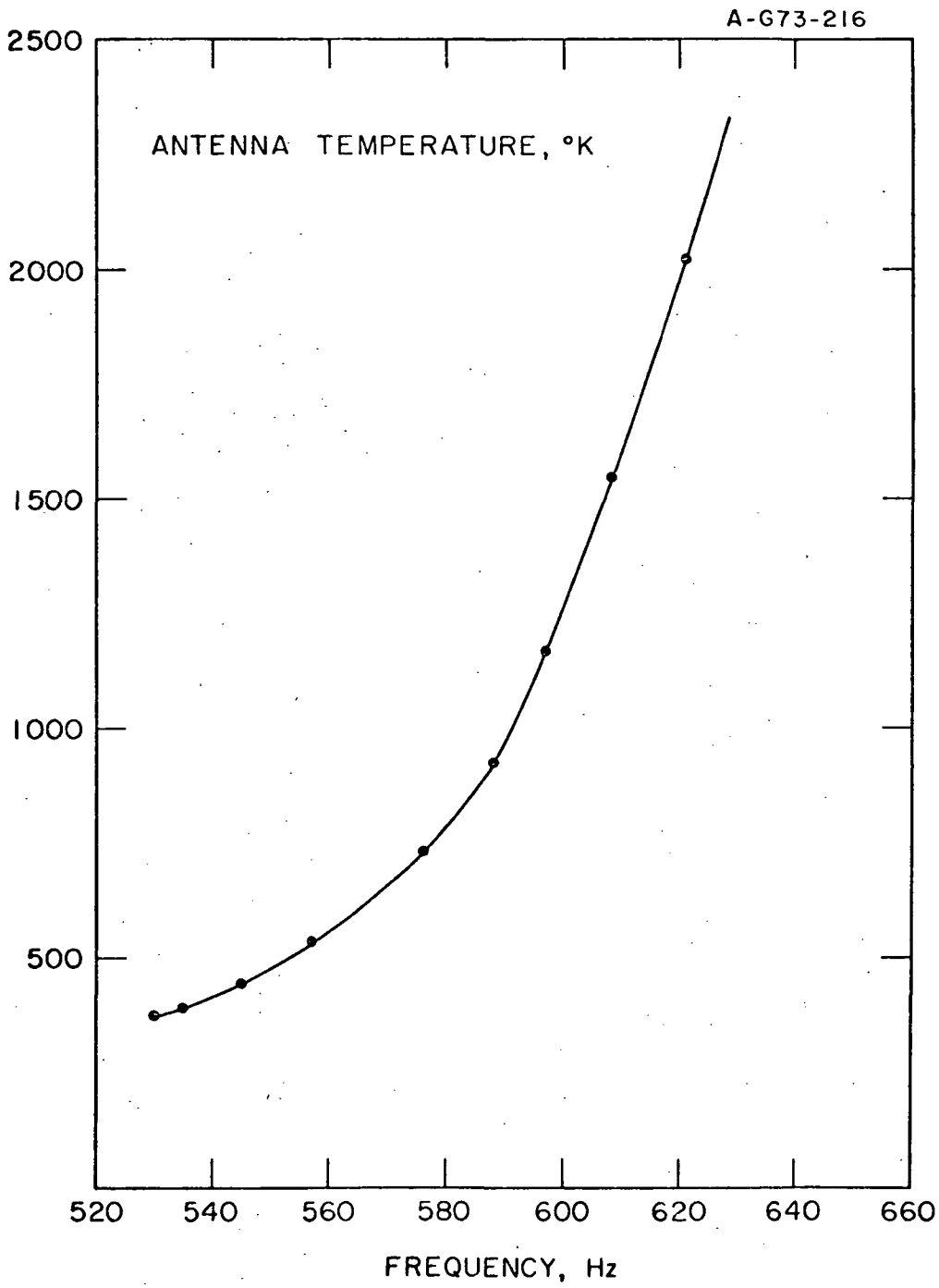
A-G73-216
ANTENNA TEMPERATURE, °K
2500
2000
1500
1000
500
520
540
560
580
600
620
640
660
FREQUENCY, Hz

Figure 2

A-G73-215

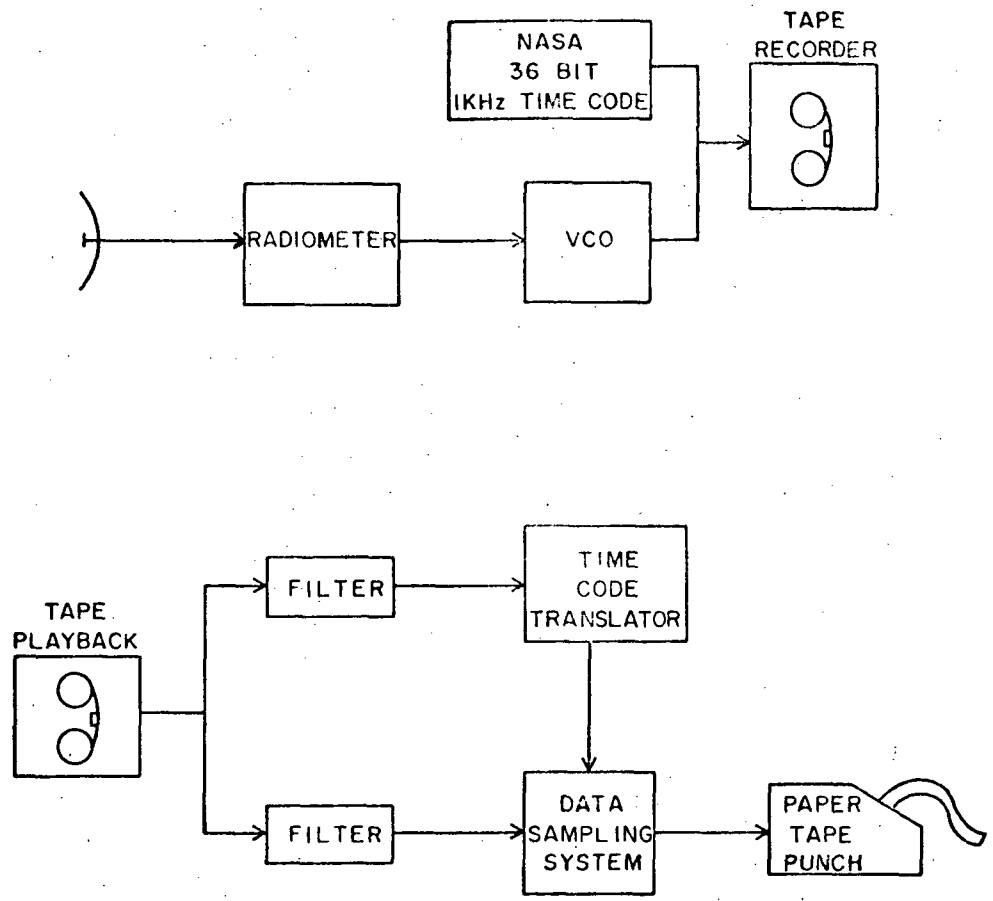

Figure 3

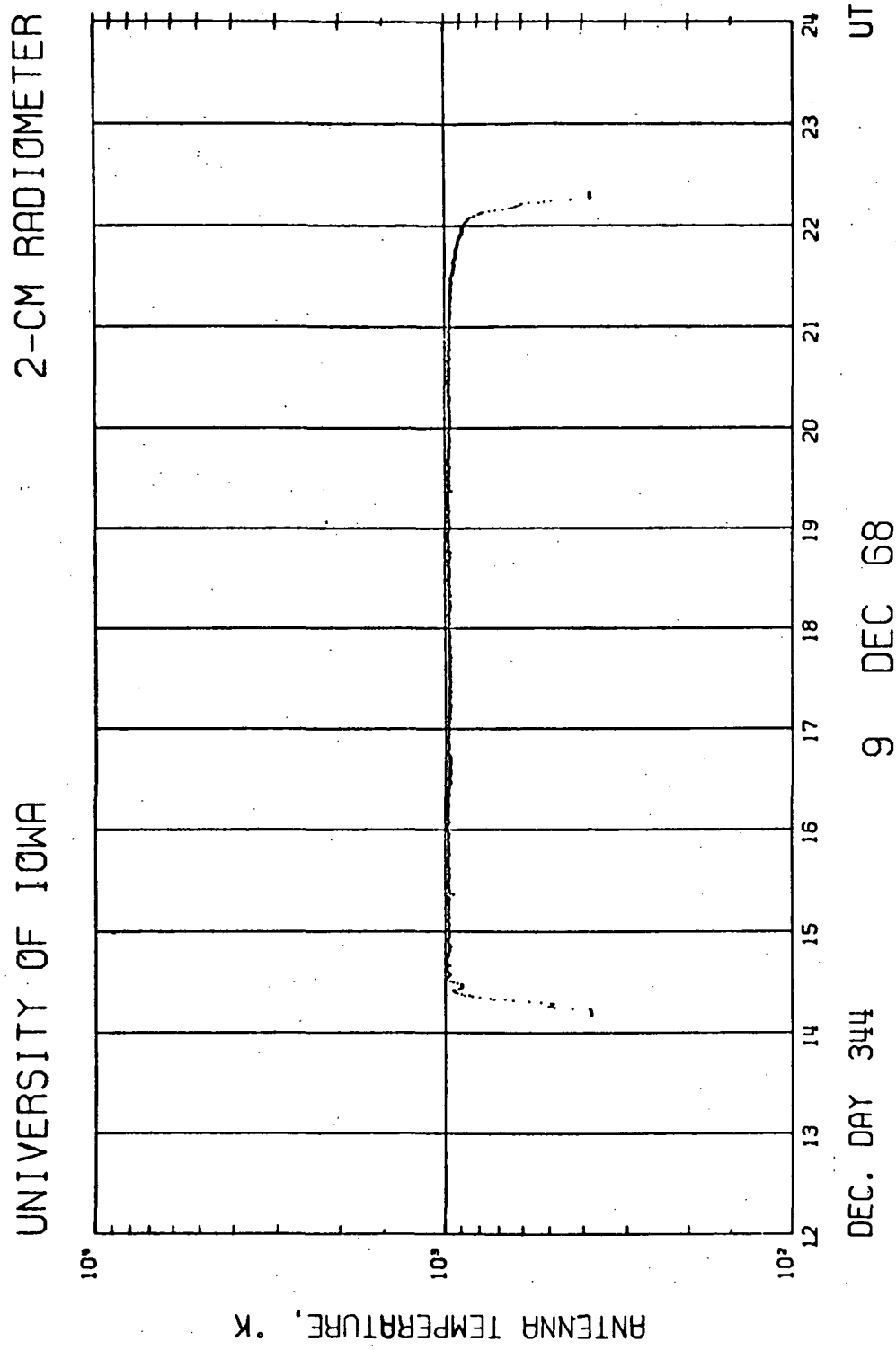
UNIVERSITY OF IOWA
2-CM RADIOMETER
ANTENNA TEMPERATURE, °K
10⁴
10³
10²
12
13
14
15
16
17
18
19
20
21
22
23
24
UT
DEC. DAY 344
9 DEC 68

Figure 4

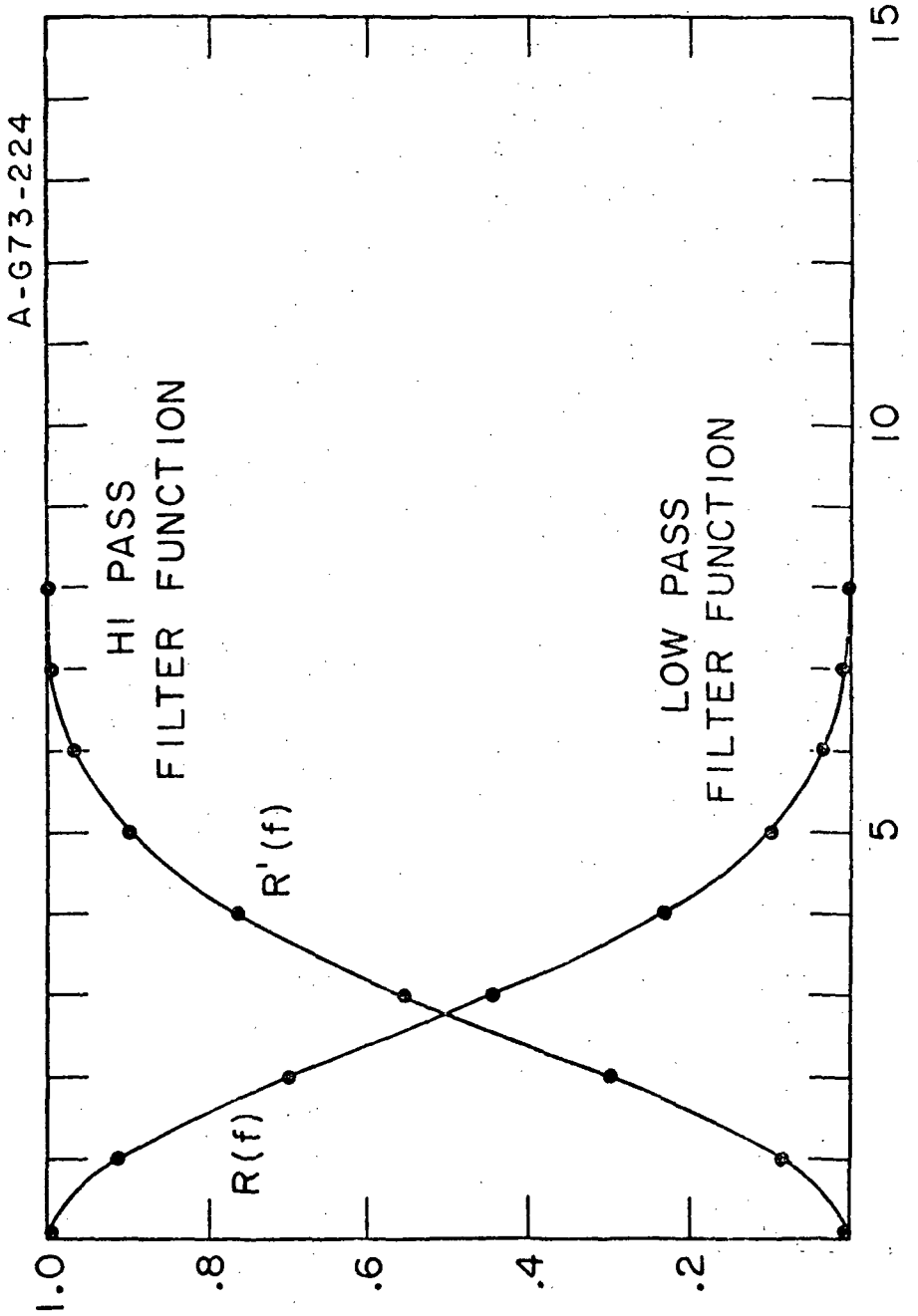
A-G73-224
HI PASS
FILTER FUNCTION
R'(f)
R(f)
LOW PASS
FILTER FUNCTION
1.0
.8
.6
.4
.2
5
10
15
FREQUENCY, mHz

Figure 5

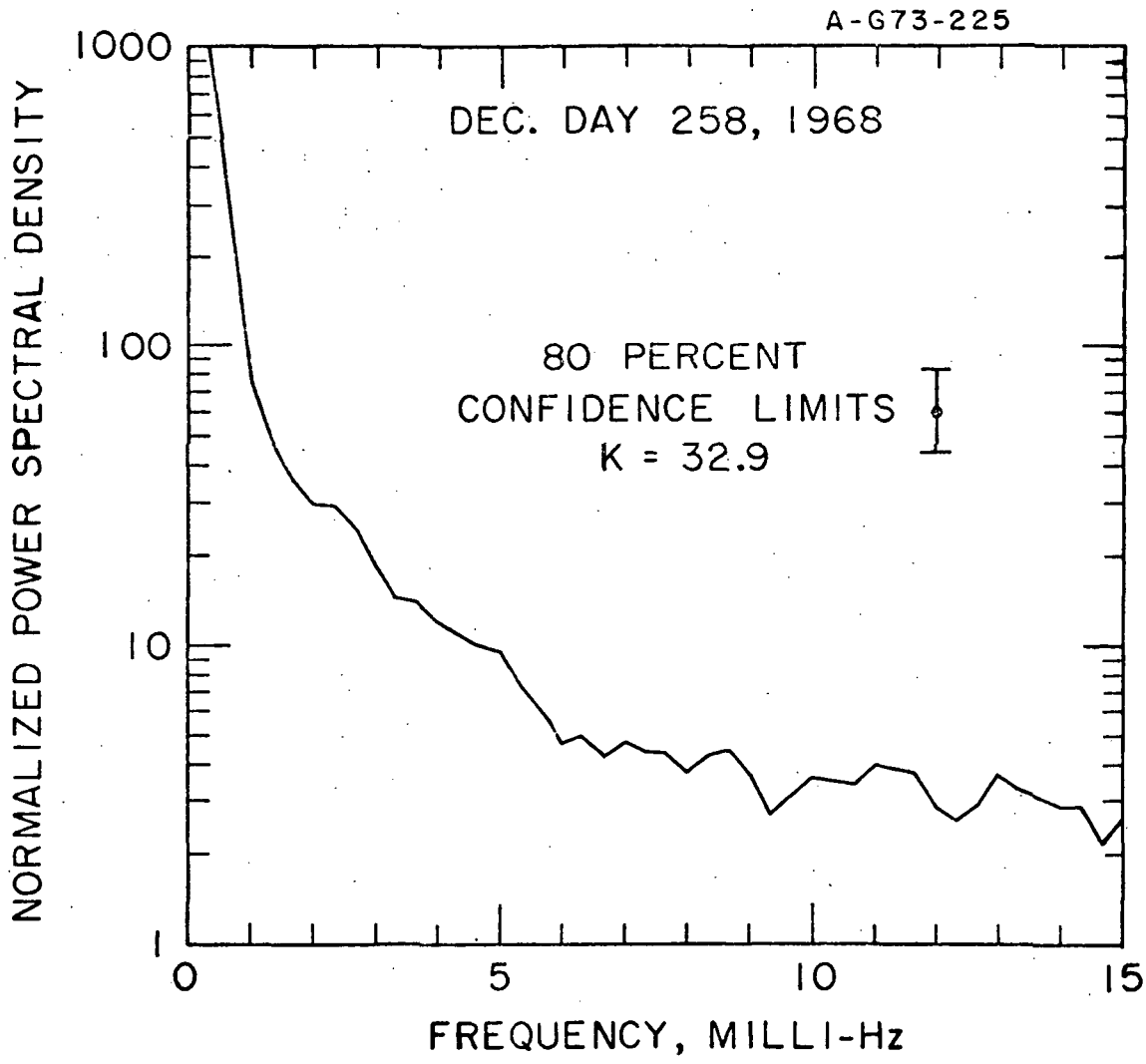
A-G73-225
DEC. DAY 258, 1968
80 PERCENT
CONFIDENCE LIMITS
K = 32.9
NORMALIZED POWER SPECTRAL DENSITY
1000
100
10
1
0
5
10
15
FREQUENCY, MILLI-Hz

Figure 6

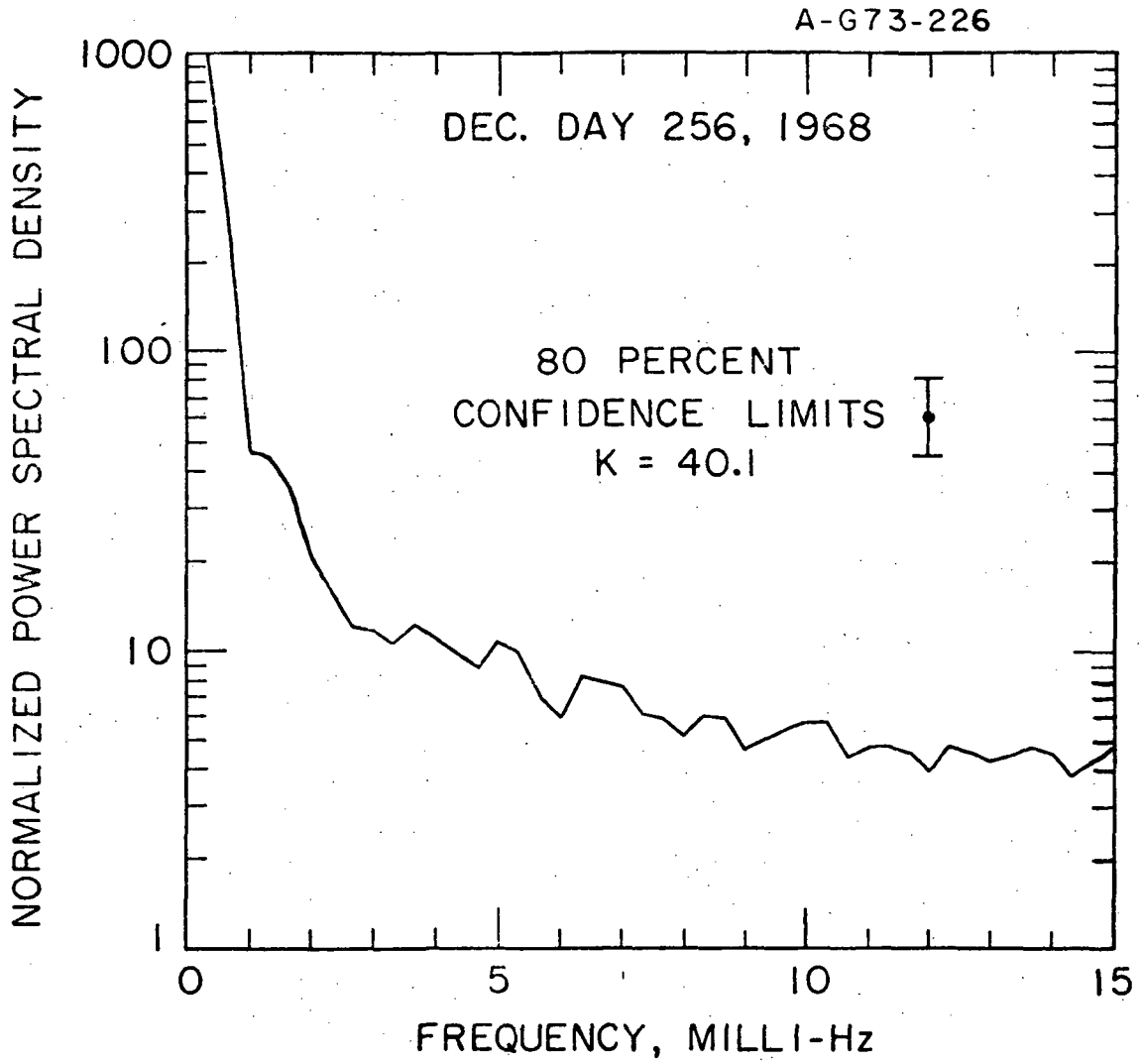
A-G73-226
DEC. DAY 256, 1968
80 PERCENT
CONFIDENCE LIMITS
K = 40.1
NORMALIZED POWER SPECTRAL DENSITY
1000
100
10
1
0
5
10
15
FREQUENCY, MILLI-Hz

Figure 7

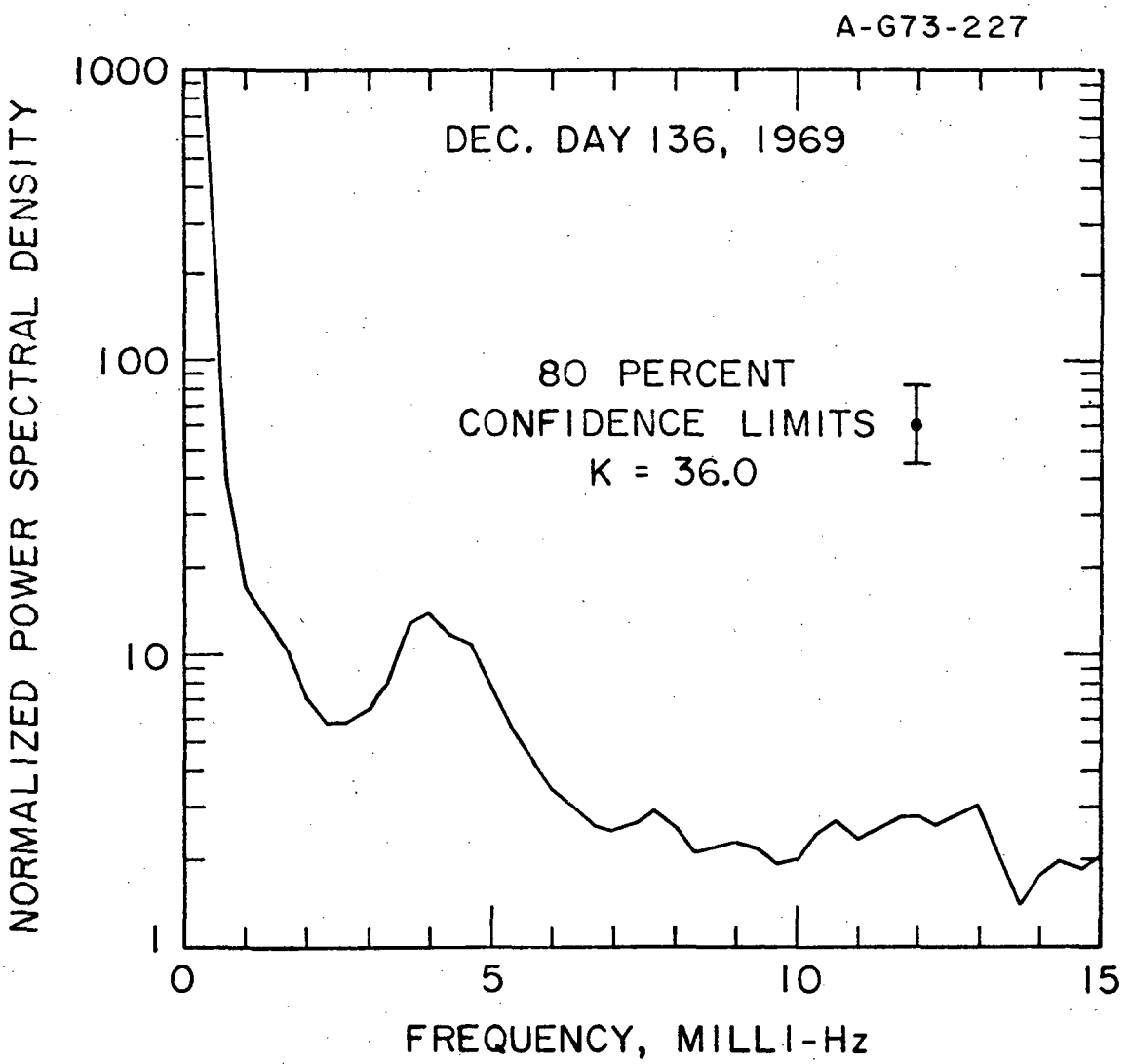
A-G73-227
DEC. DAY 136, 1969
80 PERCENT
CONFIDENCE LIMITS
K = 36.0
NORMALIZED POWER SPECTRAL DENSITY
1000
100
10
1
0
5
10
15
FREQUENCY, MILLI-Hz

Figure 8

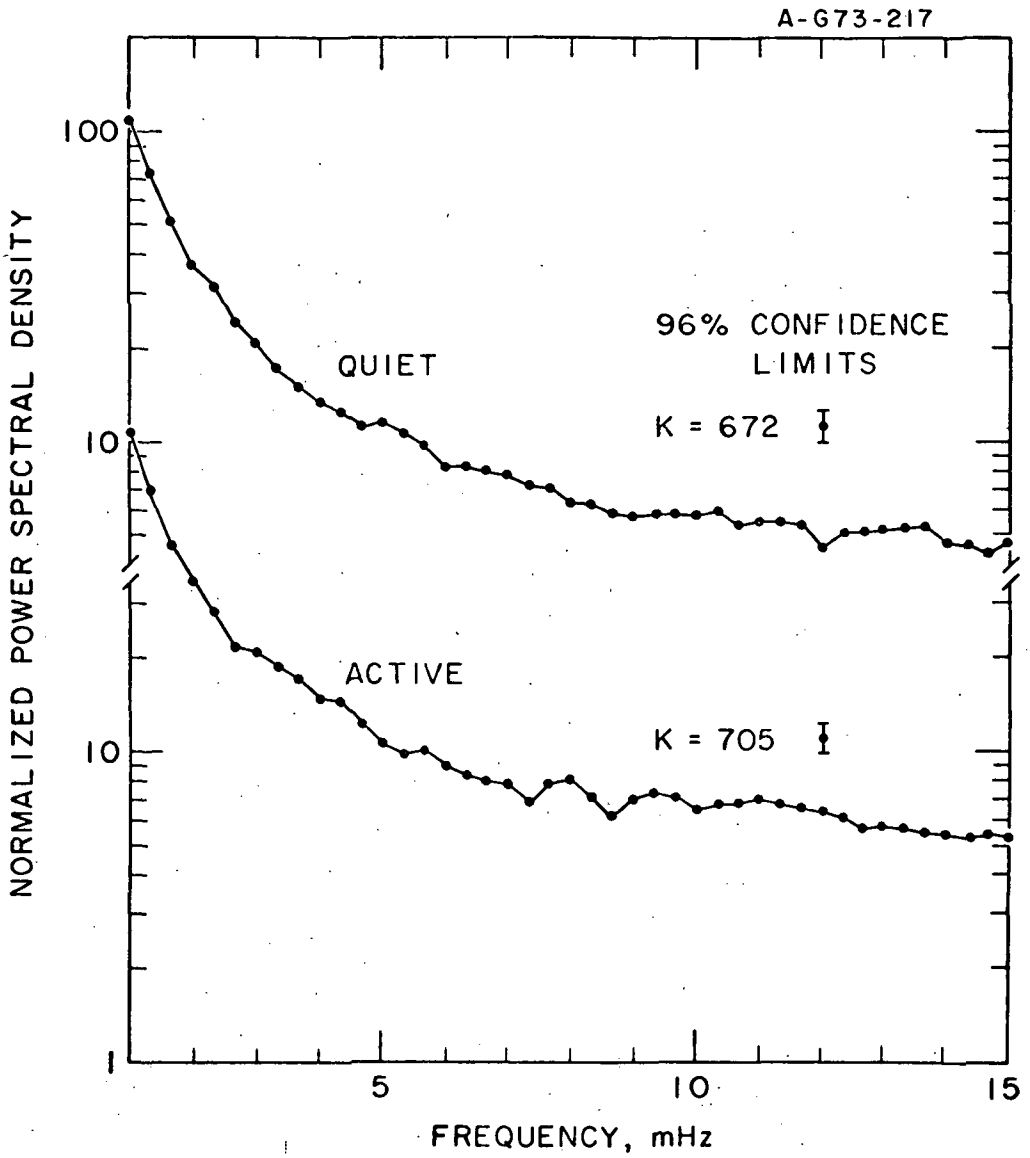
A-G73-217
NORMALIZED POWER SPECTRAL DENSITY
100
10
10
1
QUIET
96% CONFIDENCE
LIMITS
K = 672
ACTIVE
K = 705
5
10
15
FREQUENCY, mHz

Figure 9

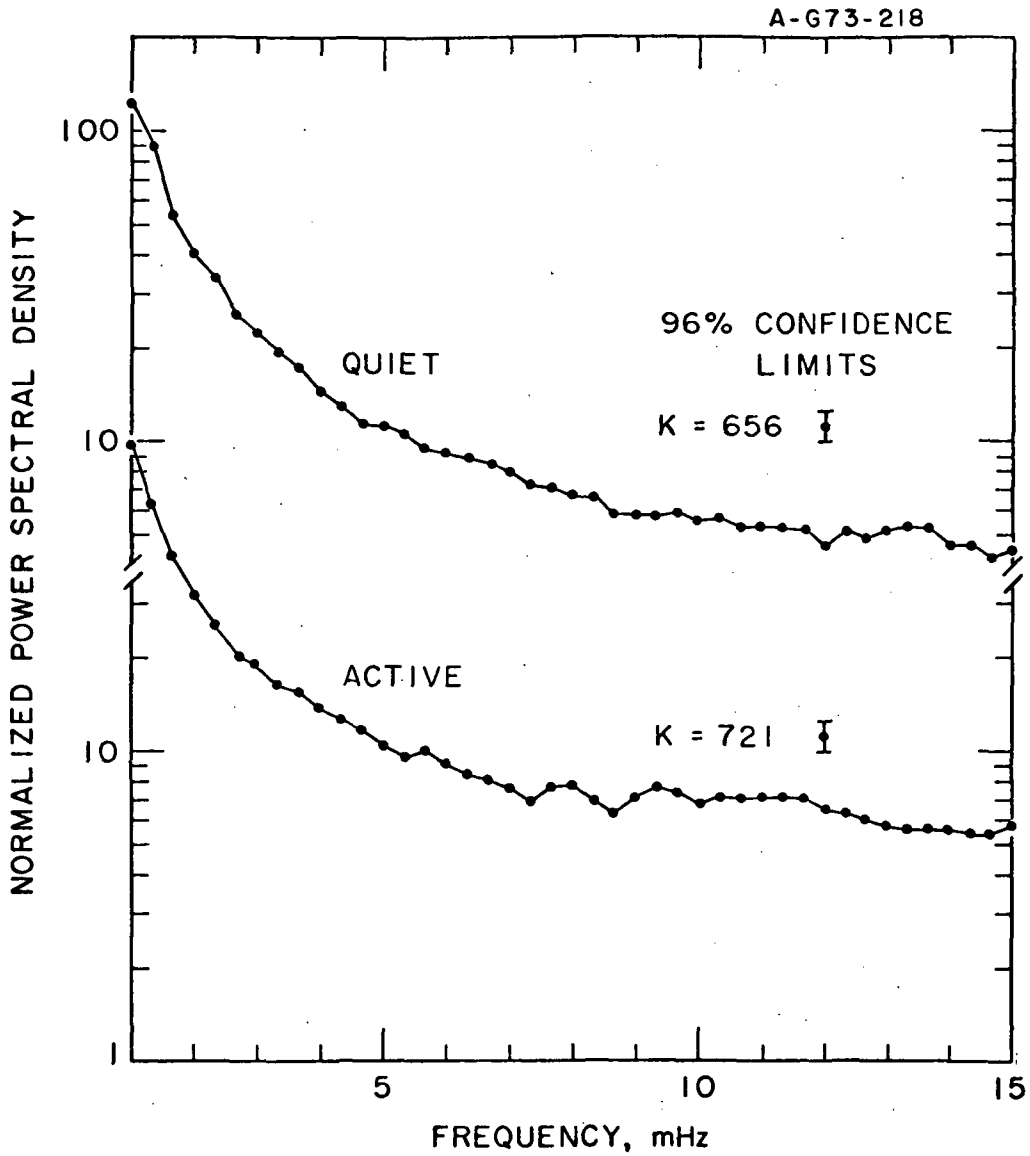
A-G73-218
NORMALIZED POWER SPECTRAL DENSITY
100
10
10
1
QUIET
96% CONFIDENCE
LIMITS
K = 656
ACTIVE
K = 721
5
10
15
FREQUENCY, mHz

Figure 10

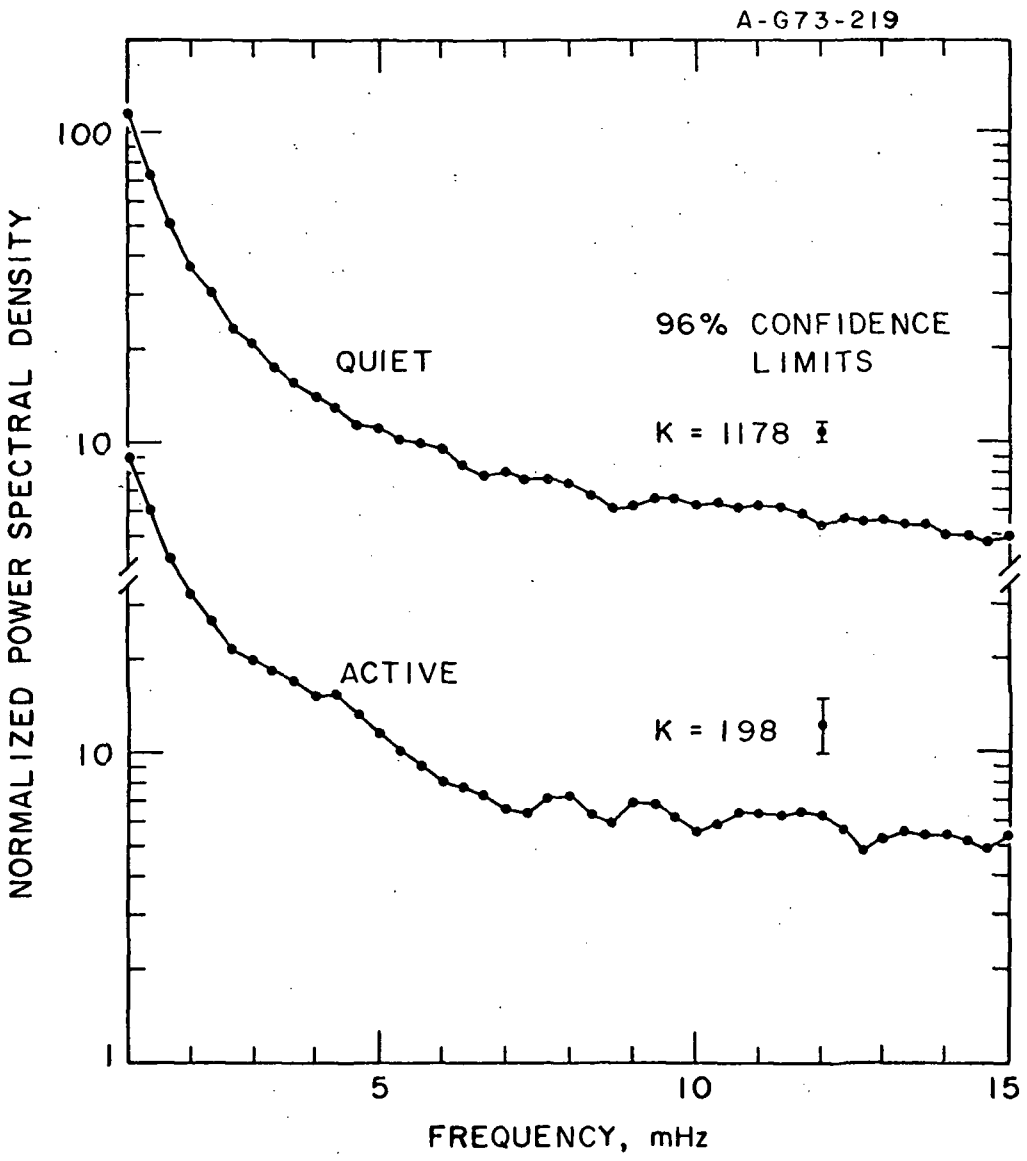
A-G73-219
NORMALIZED POWER SPECTRAL DENSITY
100
10
10
1
QUIET
96% CONFIDENCE
LIMITS
K = 1178
ACTIVE
K = 198
5
10
15
FREQUENCY, mHz

Figure 11

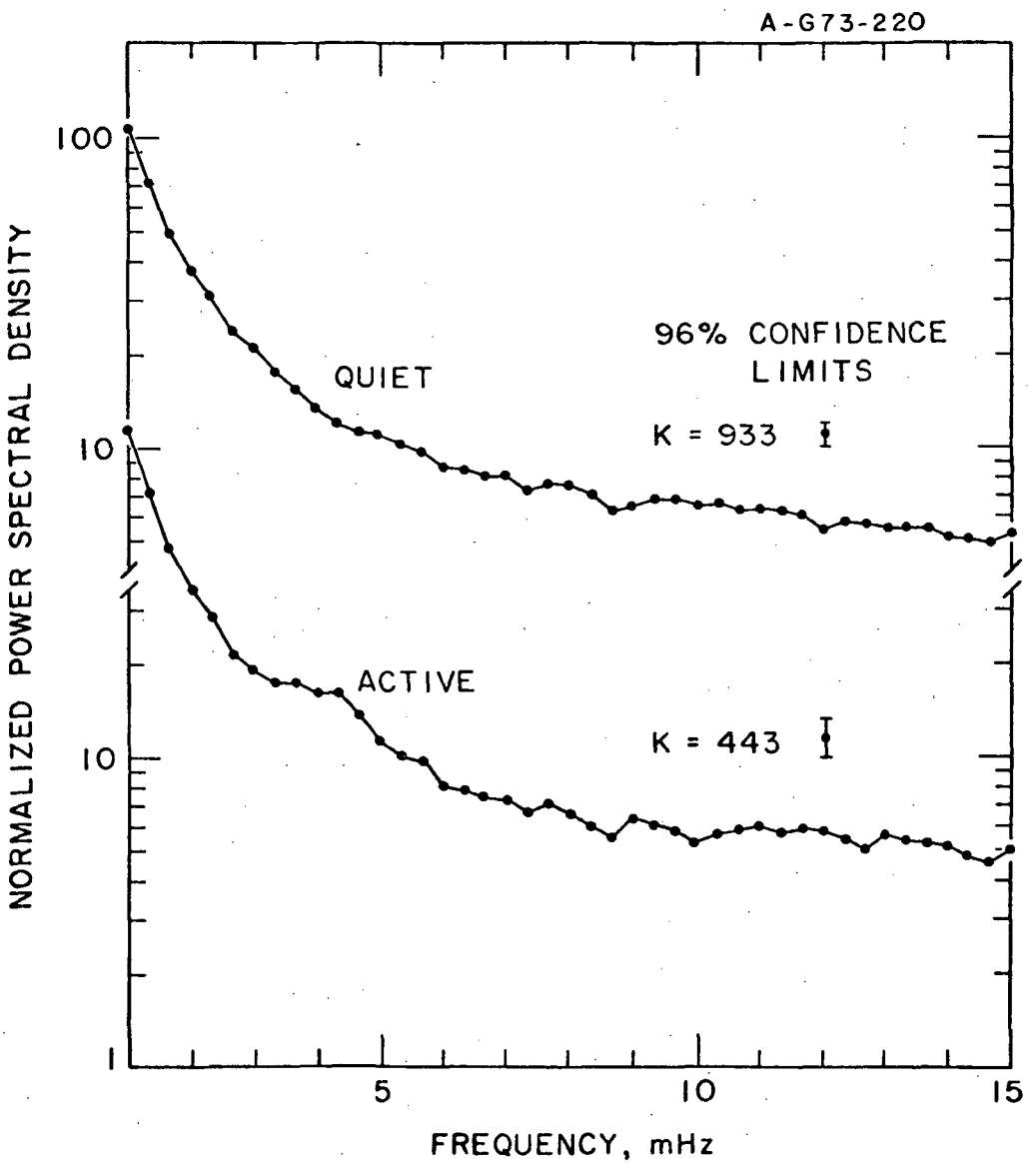
A-G73-220
100
10
10
1
NORMALIZED POWER SPECTRAL DENSITY
QUIET
96% CONFIDENCE
LIMITS
K = 933
ACTIVE
K = 443
5
10
15
FREQUENCY, mHz

Figure 12

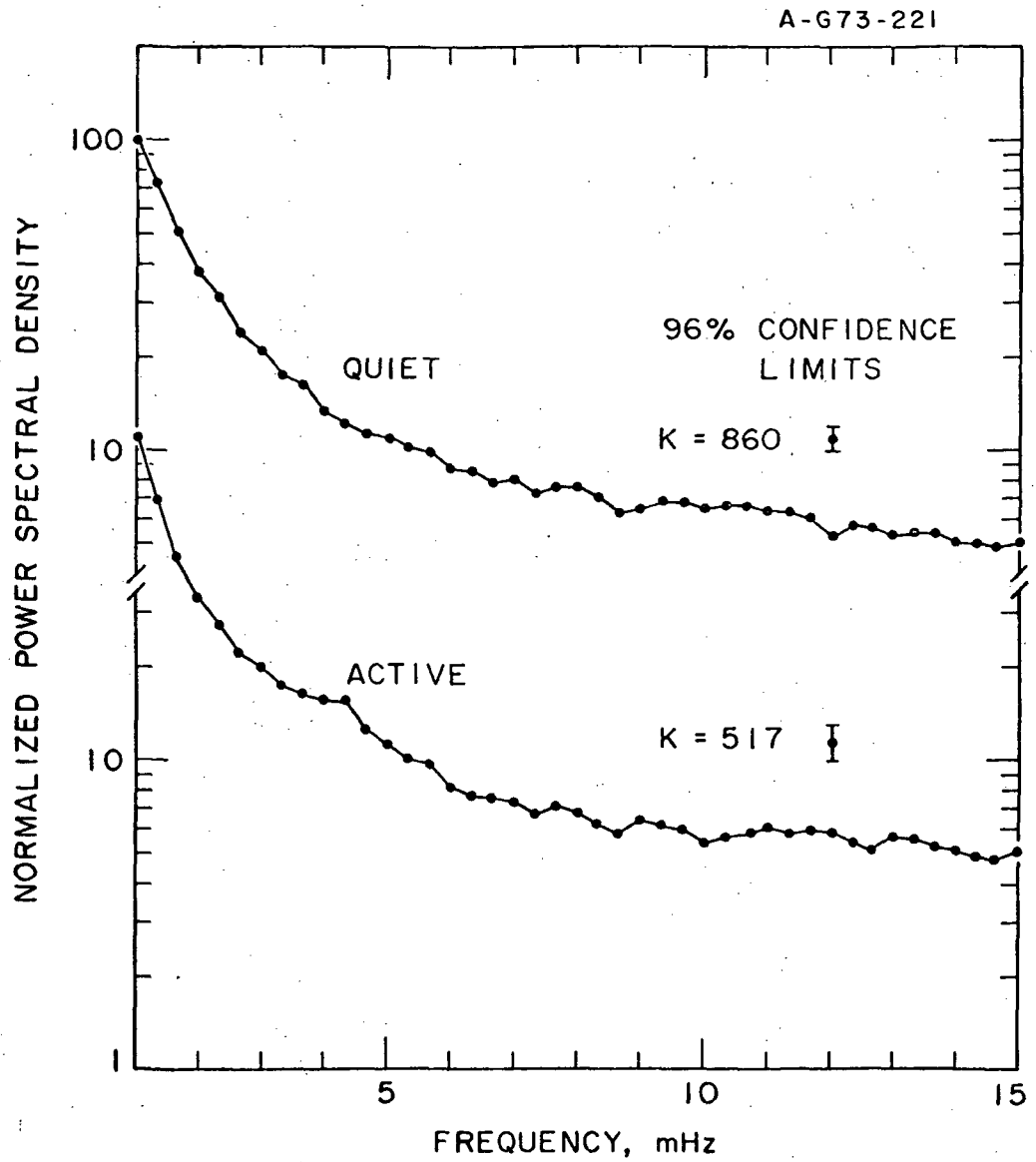
A-G73-221
NORMALIZED POWER SPECTRAL DENSITY
100
10
10
1
QUIET
96% CONFIDENCE
LIMITS
K = 860
ACTIVE
K = 517
5
10
15
FREQUENCY, mHz

Figure 13

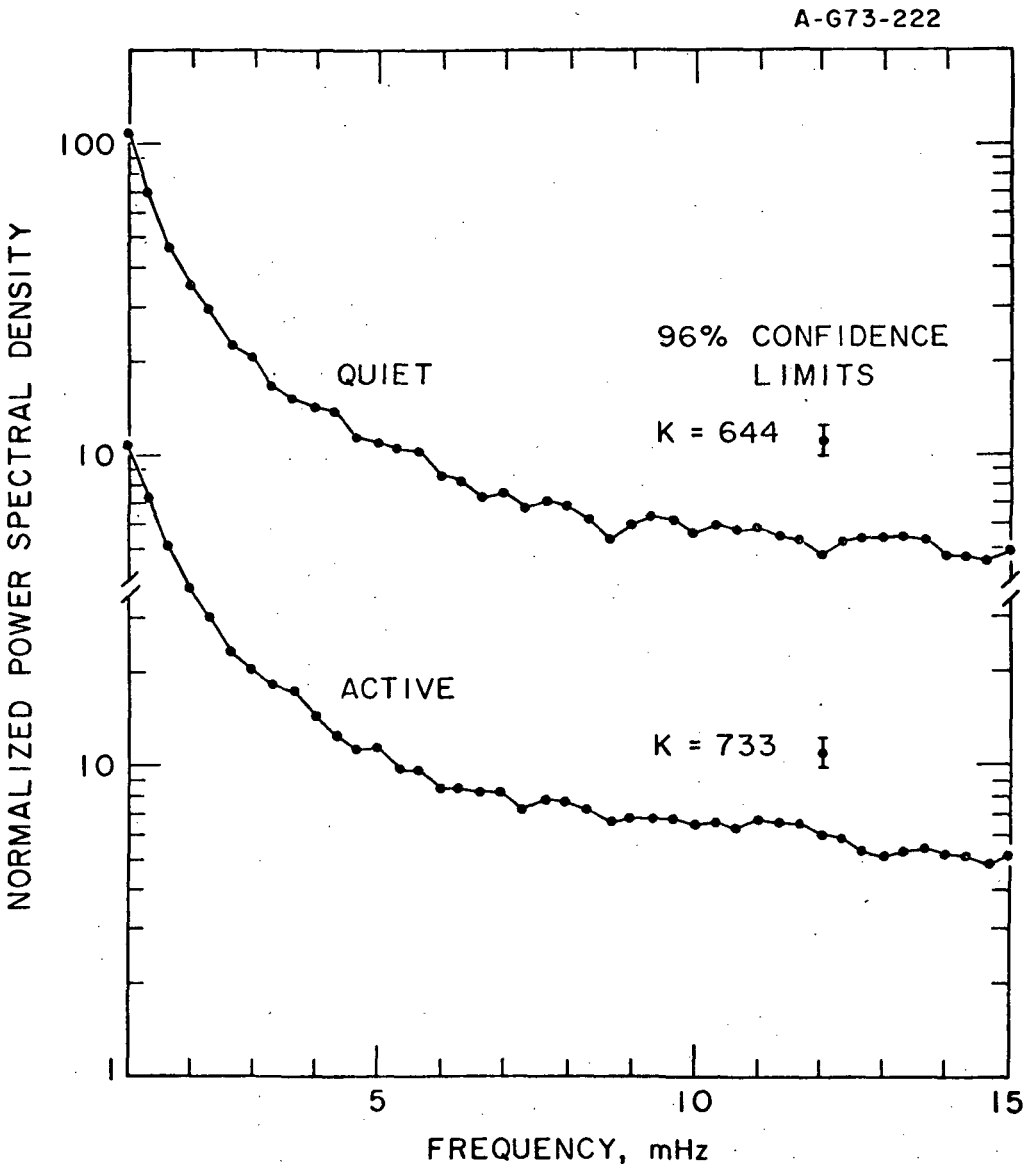
A-G73-222
100
10
10
1
NORMALIZED POWER SPECTRAL DENSITY
QUIET
96% CONFIDENCE
LIMITS
K = 644
ACTIVE
K = 733
5
10
15
FREQUENCY, mHz

Figure 14

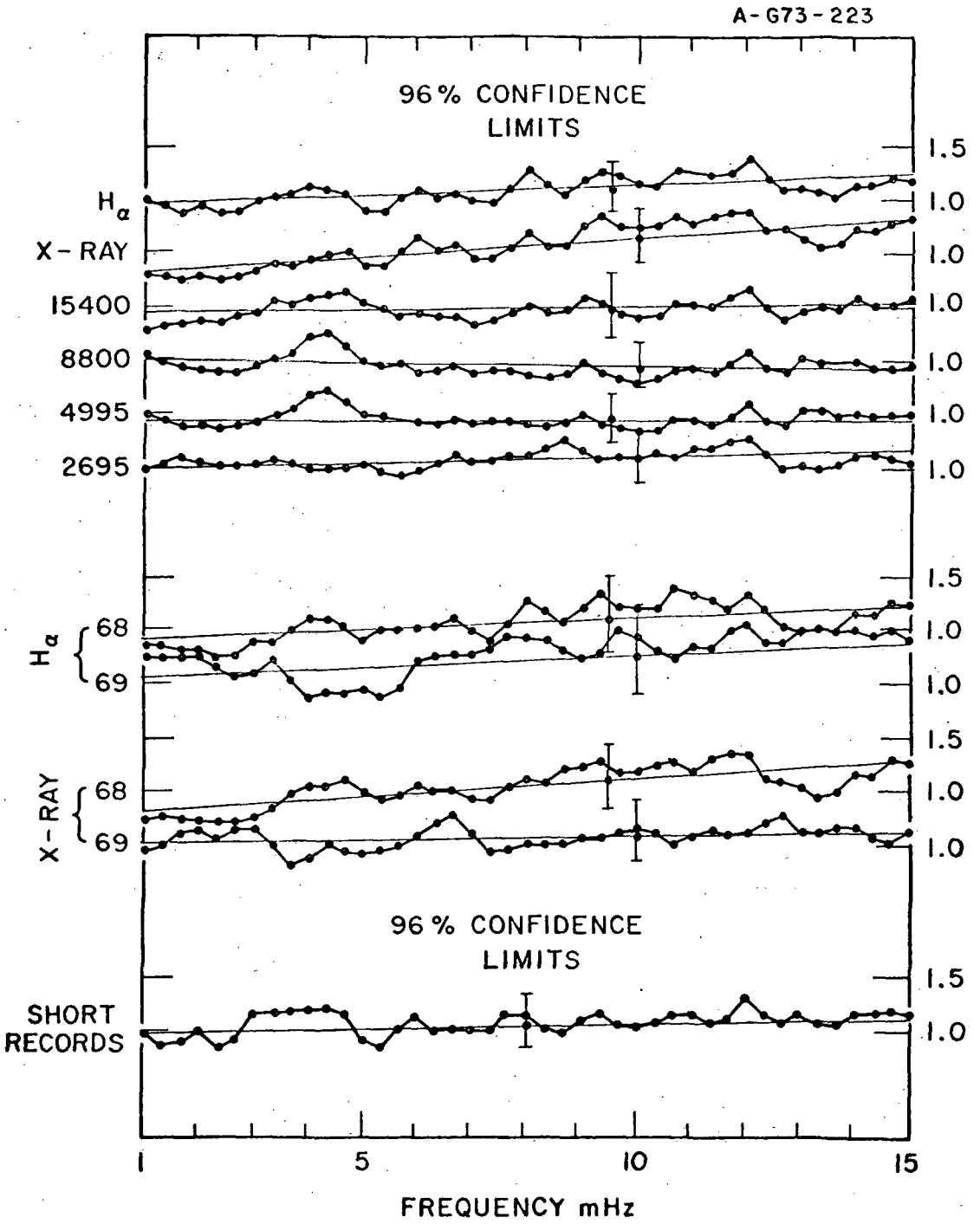
A-G73-223
96% CONFIDENCE LIMITS
H_α
X-RAY
15400
8800
4995
2695
1.5
1.0
H_α 68
69
X-RAY 68
69
96% CONFIDENCE LIMITS
SHORT RECORDS
1
5
10
15
FREQUENCY mHz

Figure 15

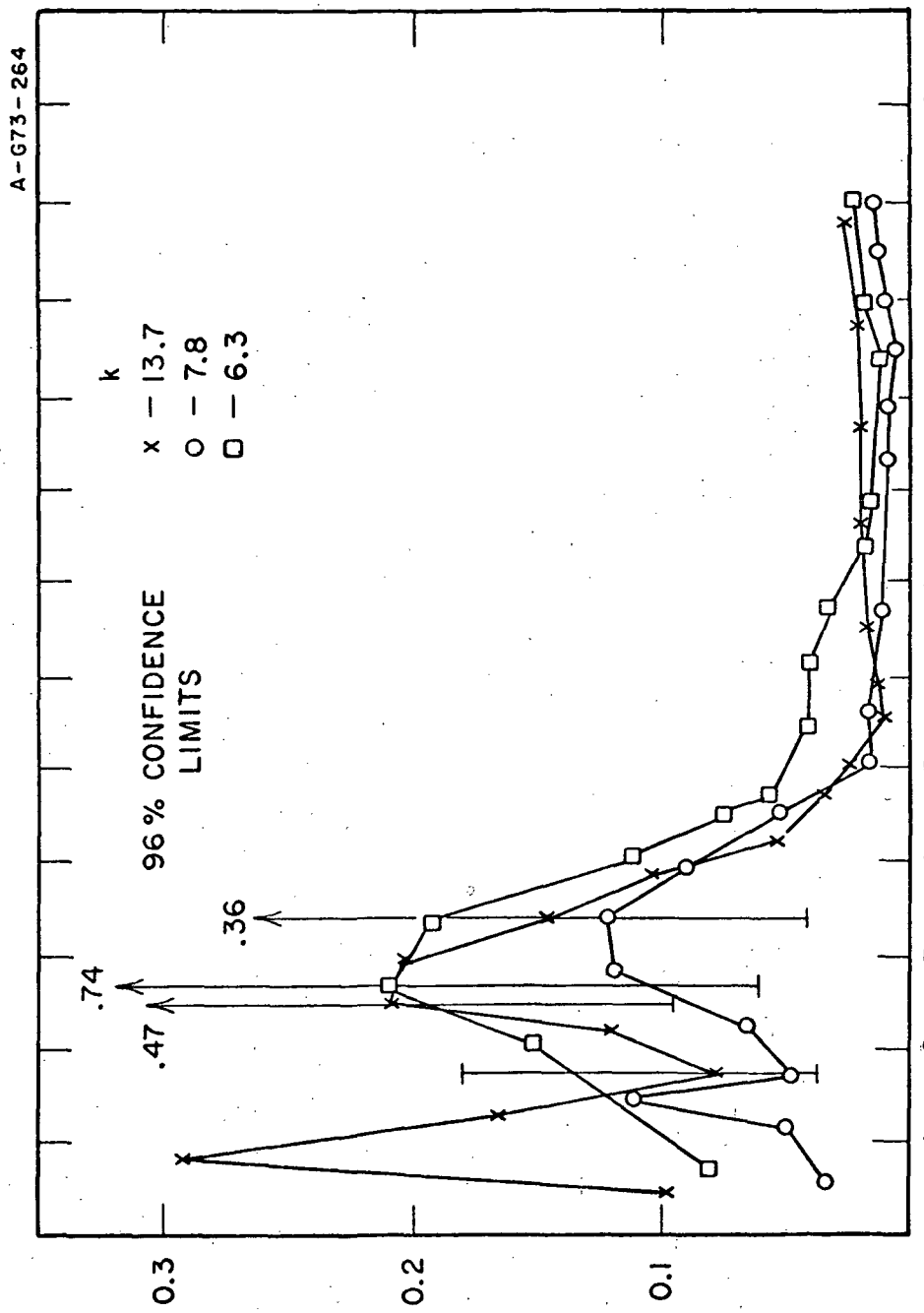
A-G73-264
k
x — 13.7
o — 7.8
□ — 6.3
96% CONFIDENCE
LIMITS
.74
.47
.36
0.3
0.2
0.1
1
2
3
4
5
6
7
8
9
10
11
12
FREQUENCY, mHz

Figure 16

A-G73-260

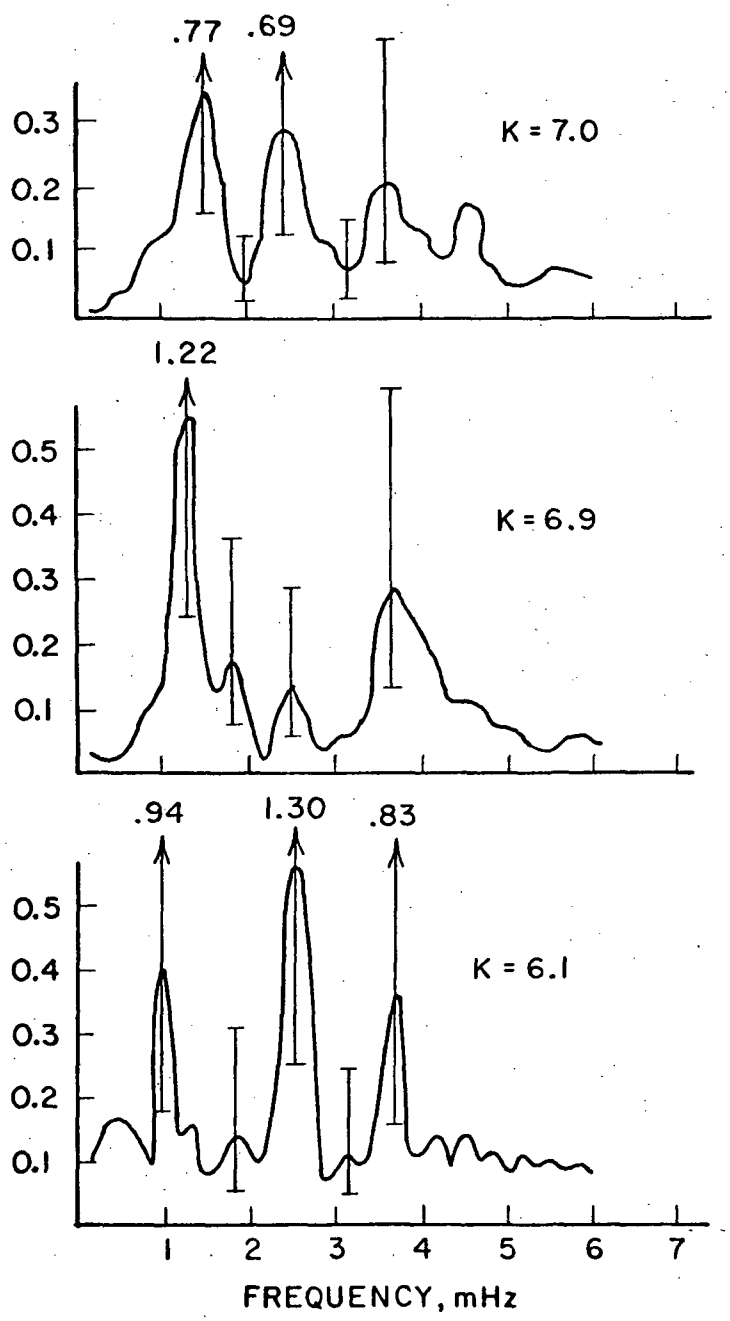

Figure 17

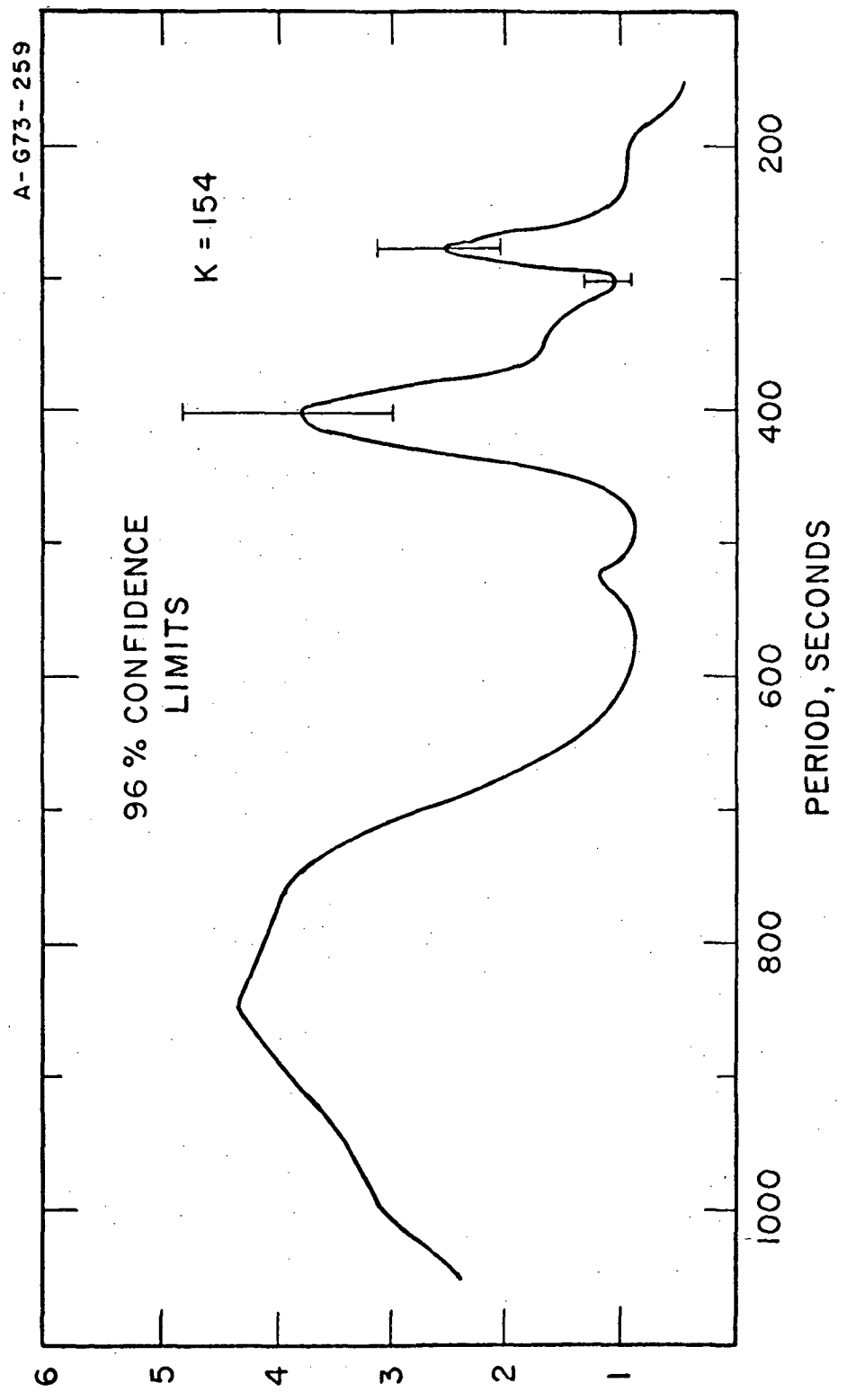
A-G73-259
K = 154
96 % CONFIDENCE LIMITS
PERIOD, SECONDS
200
400
600
800
1000
1
2
3
4
5
6

Figure 18

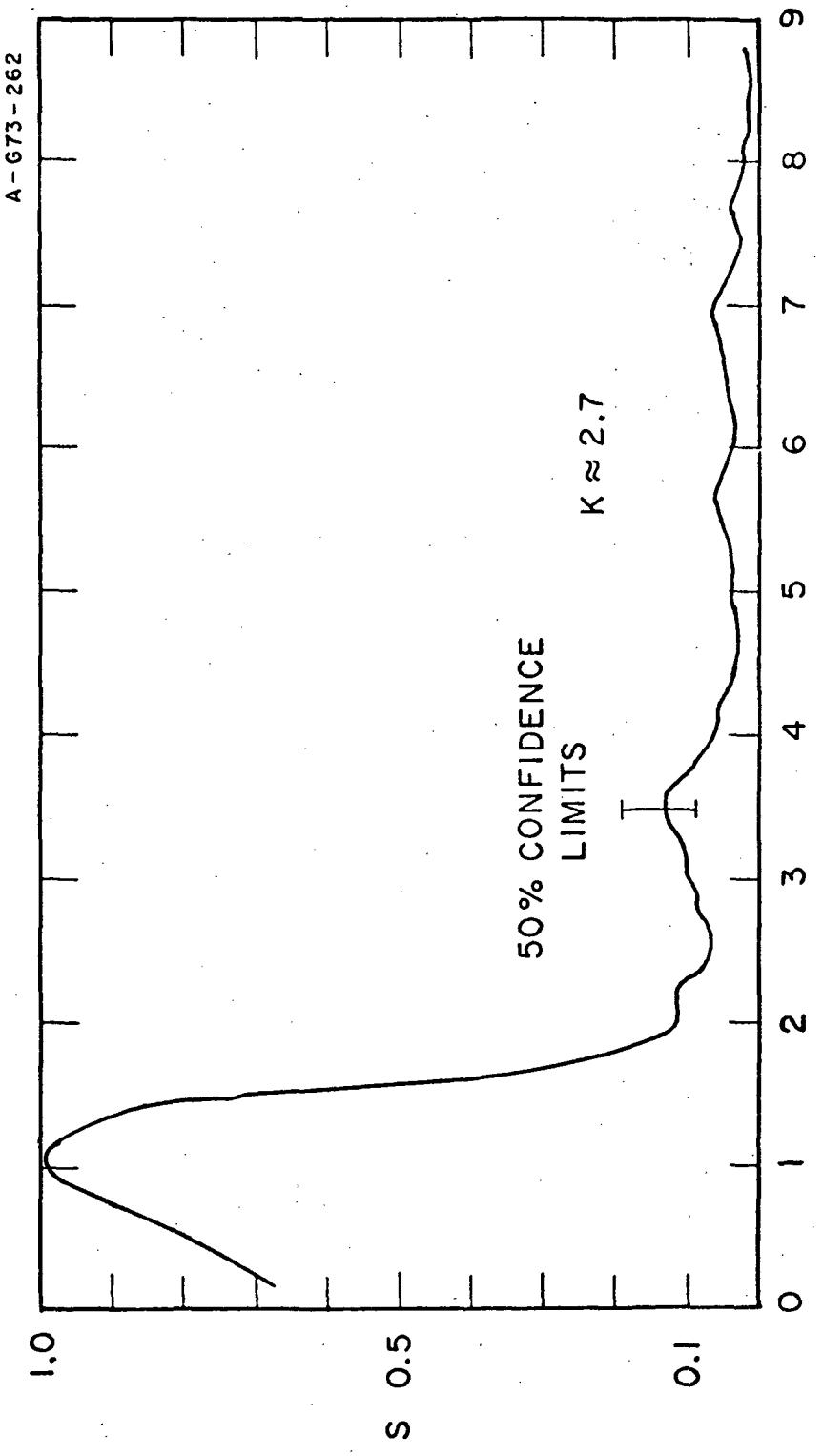
A-673-262
1.0
S 0.5
0.1
0
1
2
3
4
5
6
7
8
9
FREQUENCY, mHz
50% CONFIDENCE
LIMITS
K ≈ 2.7

Figure 19

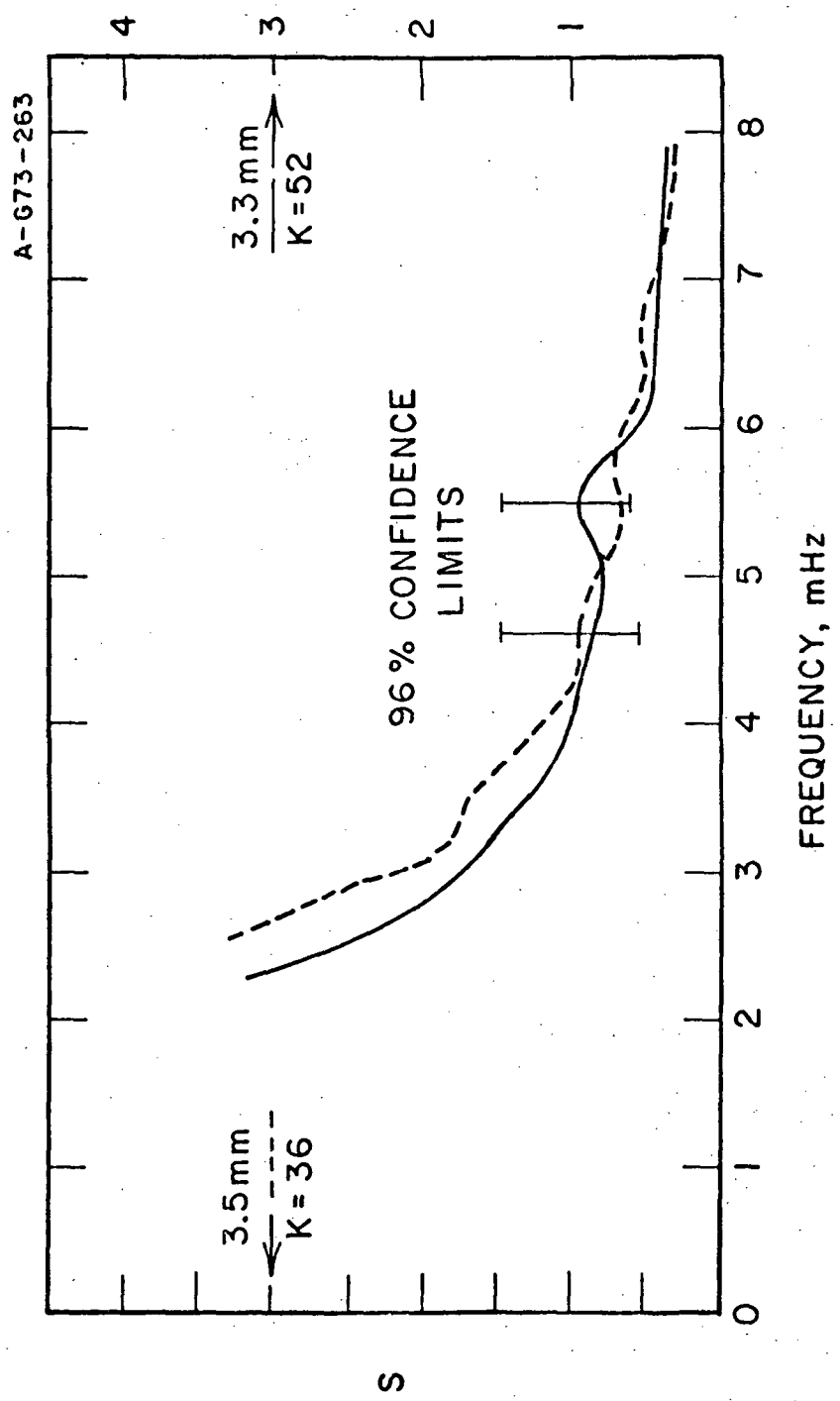
A-673-263
3.3mm
K=52
3.5mm
K=36
96% CONFIDENCE
LIMITS
FREQUENCY, mHz
S
0
1
2
3
4
5
6
7
8
1
2
3
4

Figure 20

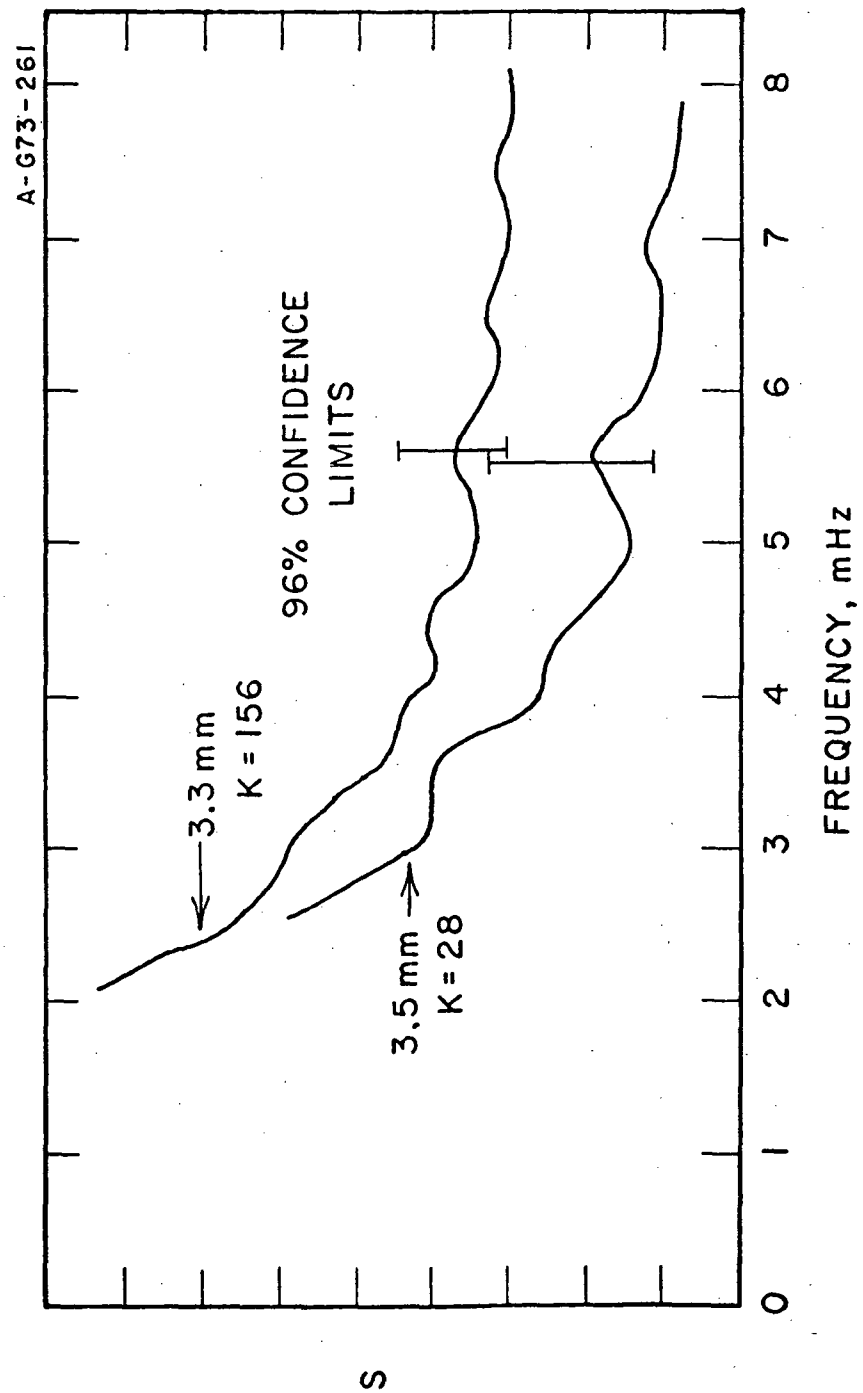
A-G73-261
S
0
1
2
3
4
5
6
7
8
FREQUENCY, mHz
3.3 mm
K = 156
3.5 mm
K = 28
96% CONFIDENCE
LIMITS

Figure 21

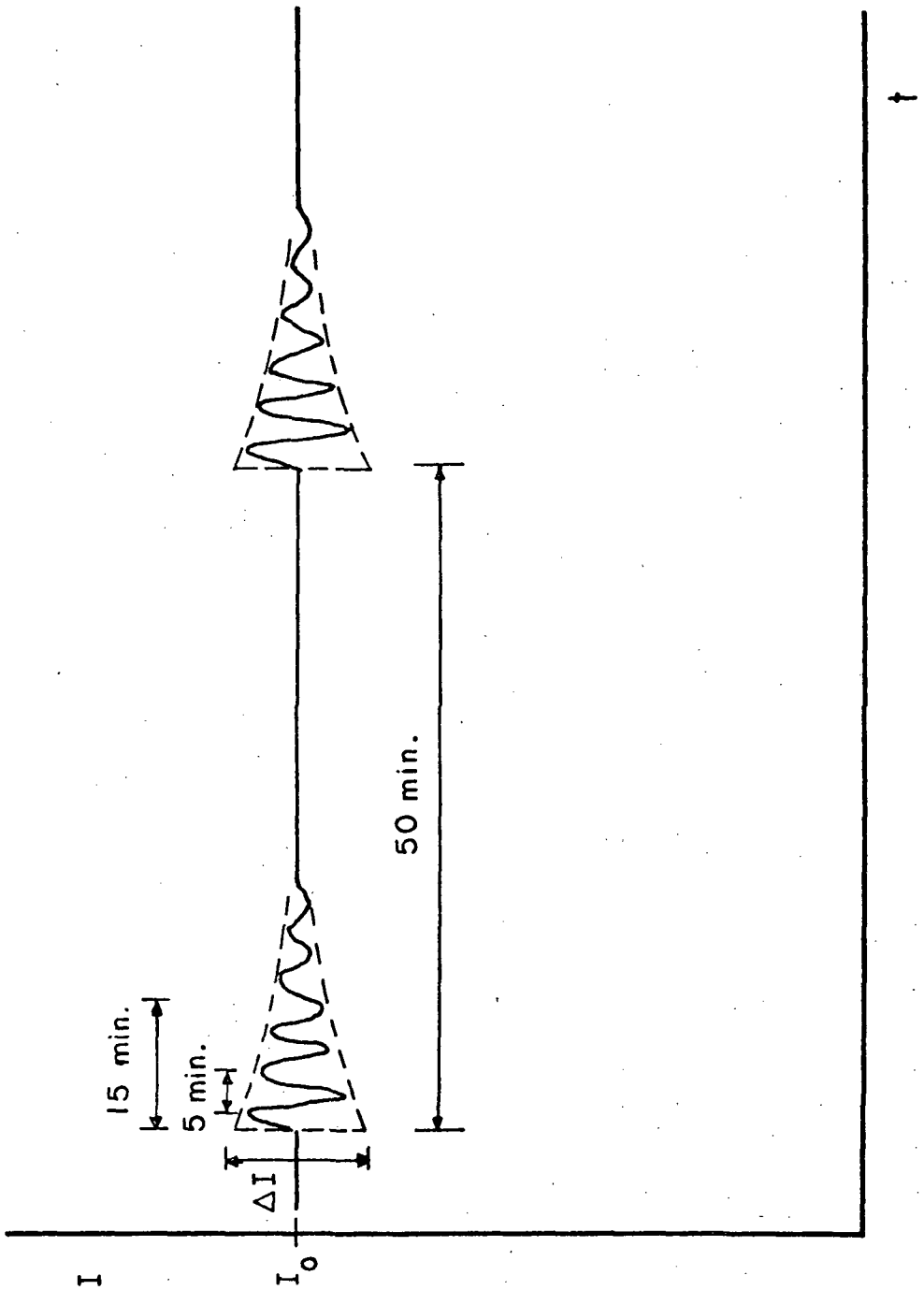

Figure 22

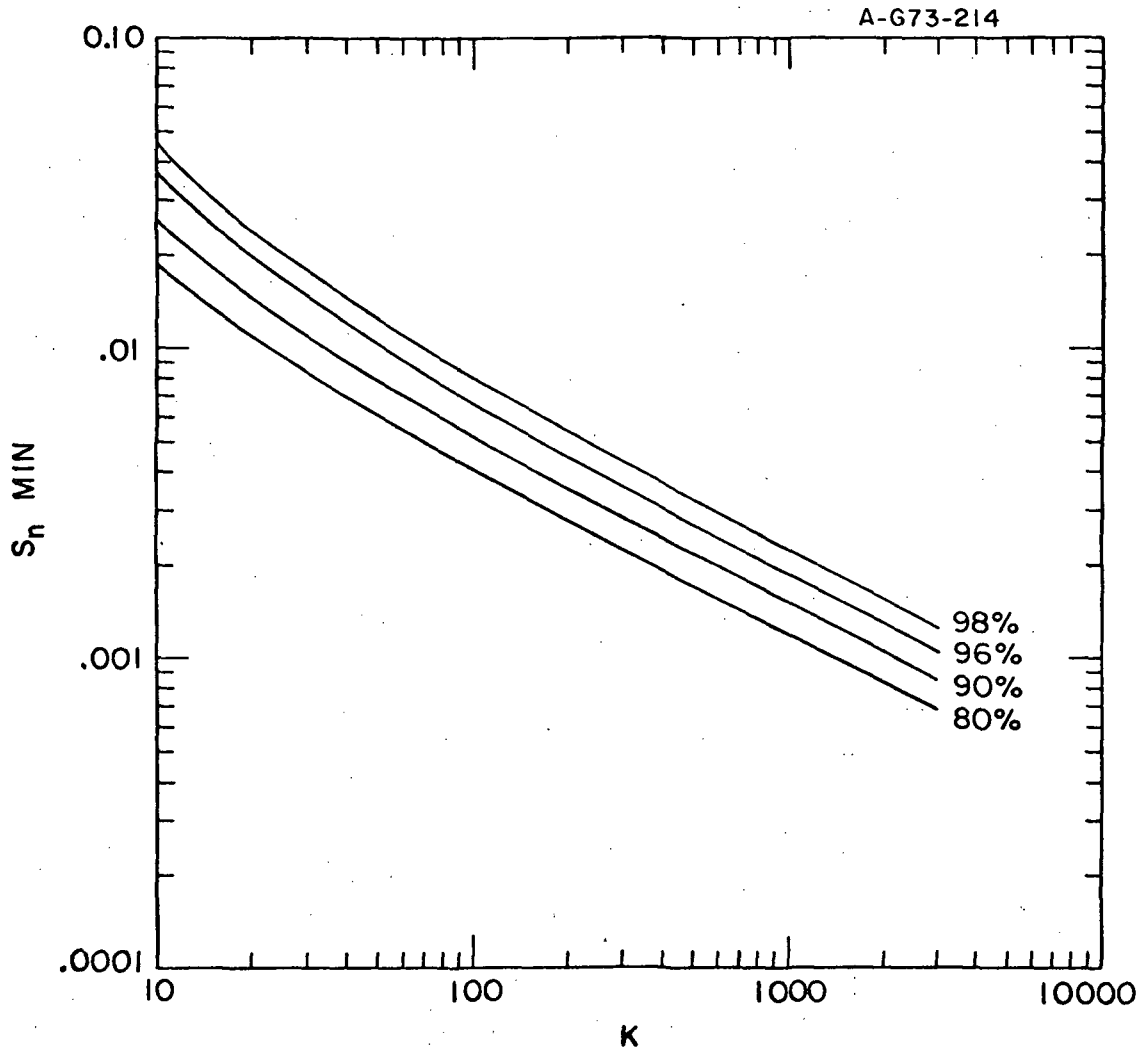

Figure 23

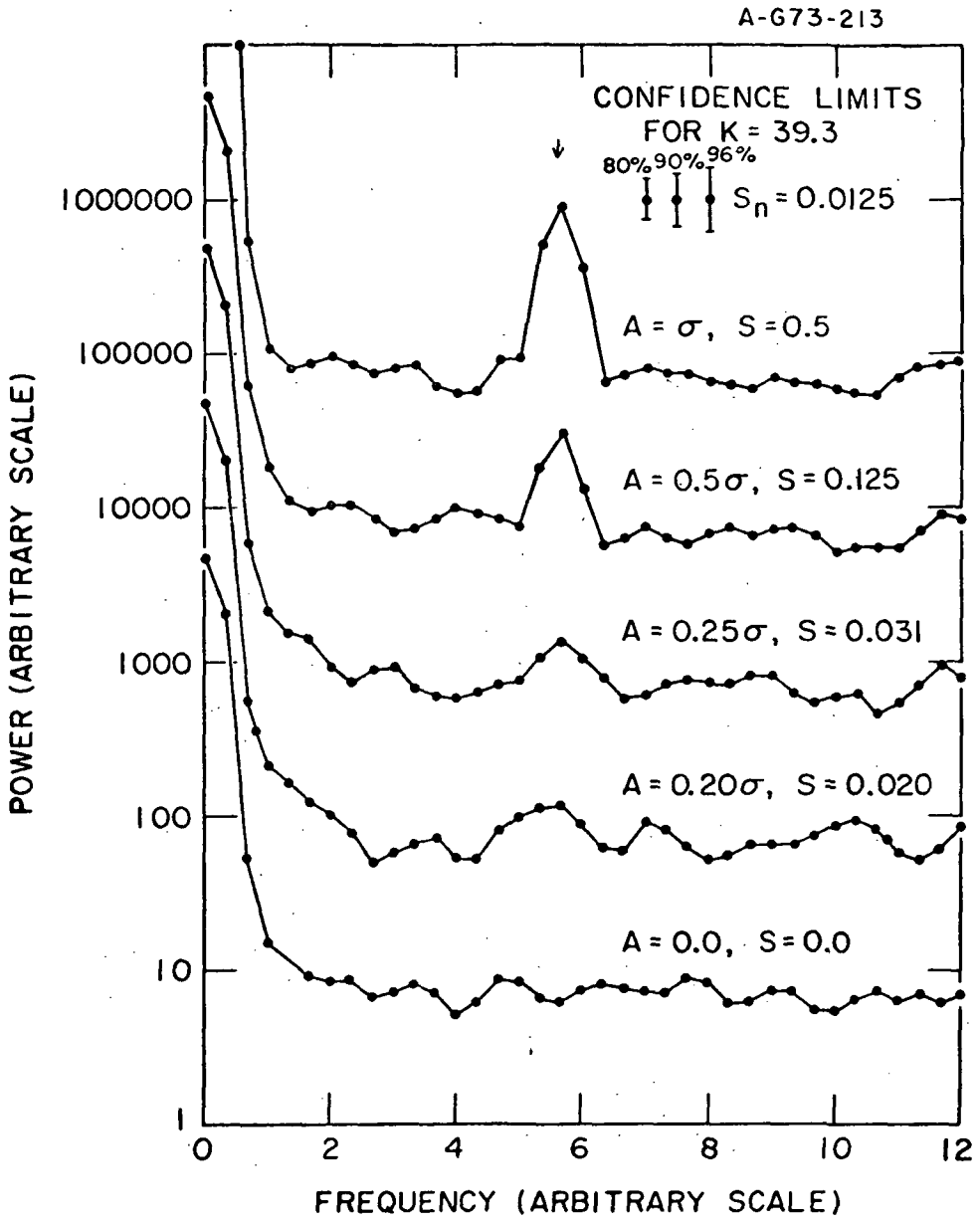
A-G73-213
CONFIDENCE LIMITS
FOR K = 39.3
80% 90% 96%
S_n = 0.0125
A = σ, S = 0.5
A = 0.5σ, S = 0.125
A = 0.25σ, S = 0.031
A = 0.20σ, S = 0.020
A = 0.0, S = 0.0
POWER (ARBITRARY SCALE)
1000000
100000
10000
1000
100
10
1
0
2
4
6
8
10
12
FREQUENCY (ARBITRARY SCALE)

Figure 24

UNCLASSIFIED

Security Classification

DOCUMENT CONTROL DATA - R&D

(Security classification of title, body of abstract and indexing annotation must be entered when the overall report is classified)

1 ORIGINATING ACTIVITY (Corporate author)	2a. REPORT SECURITY CLASSIFICATION
Department of Physics and Astronomy The University of Iowa	UNCLASSIFIED
	2b. GROUP

3. REPORT TITLE

A Search for Periodic Structure in Solar 2 cm Microwave Radiation

4. DESCRIPTIVE NOTES (Type of report and inclusive dates)

Thesis (M.S.)

5 AUTHOR(S) (Last name, first name, initial)

Sentman, Davis D.

6. REPORT DATE	7a. TOTAL NO. OF PAGES	7b. NO. OF REFS
May 1973	85	26

8a. CONTRACT OR GRANT NO.	9a. ORIGINATOR'S REPORT NUMBER(S)
N00014-68-A-0196-0003	U. of Iowa 73-20
b. PROJECT NO.	
c.	9b. OTHER REPORT NO(S) (Any other numbers that may be assigned this report)
d.	

10. AVAILABILITY/LIMITATION NOTICES

Distribution of this document is unlimited.

11. SUPPLEMENTARY NOTES	12. SPONSORING MILITARY ACTIVITY
	Office of Naval Research

13. ABSTRACT

See following pages.

DD FORM 1 JAN 64 1473

UNCLASSIFIED

Security Classification

14. KEY WORDS	LINK A		LINK B		LINK C	
	ROLE	WT	ROLE	WT	ROLE	WT
Solar microwaves						
Periodicities						
Power spectrum						

INSTRUCTIONS

1. ORIGINATING ACTIVITY: Enter the name and address of the contractor, subcontractor, grantee, Department of Defense activity or other organization *(corporate author)* issuing the report.

2a. REPORT SECURITY CLASSIFICATION: Enter the overall security classification of the report. Indicate whether "Restricted Data" is included. Marking is to be in accordance with appropriate security regulations.

2b. GROUP: Automatic downgrading is specified in DoD Directive 5200.10 and Armed Forces Industrial Manual. Enter the group number. Also, when applicable, show that optional markings have been used for Group 3 and Group 4 as authorized.

3. REPORT TITLE: Enter the complete report title in all capital letters. Titles in all cases should be unclassified. If a meaningful title cannot be selected without classification, show title classification in all capitals in parenthesis immediately following the title.

4. DESCRIPTIVE NOTES: If appropriate, enter the type of report, e.g., interim, progress, summary, annual, or final. Give the inclusive dates when a specific reporting period is covered.

5. AUTHOR(S): Enter the name(s) of author(s) as shown on or in the report. Enter last name, first name, middle initial. If military, show rank and branch of service. The name of the principal author is an absolute minimum requirement.

6. REPORT DATE: Enter the date of the report as day, month, year; or month, year. If more than one date appears on the report, use date of publication.

7a. TOTAL NUMBER OF PAGES: The total page count should follow normal pagination procedures, i.e., enter the number of pages containing information.

7b. NUMBER OF REFERENCES: Enter the total number of references cited in the report.

8a. CONTRACT OR GRANT NUMBER: If appropriate, enter the applicable number of the contract or grant under which the report was written.

8b, 8c, & 8d. PROJECT NUMBER: Enter the appropriate military department identification, such as project number, subproject number, system numbers, task number, etc.

9a. ORIGINATOR'S REPORT NUMBER(S): Enter the official report number by which the document will be identified and controlled by the originating activity. This number must be unique to this report.

9b. OTHER REPORT NUMBER(S): If the report has been assigned any other report numbers *(either by the originator or by the sponsor)*, also enter this number(s).

10. AVAILABILITY/LIMITATION NOTICES: Enter any limitations on further dissemination of the report, other than those imposed by security classification, using standard statements such as:

(1) "Qualified requesters may obtain copies of this report from DDC."

(2) "Foreign announcement and dissemination of this report by DDC is not authorized."

(3) "U. S. Government agencies may obtain copies of this report directly from DDC. Other qualified DDC users shall request through _____."

(4) "U. S. military agencies may obtain copies of this report directly from DDC. Other qualified users shall request through _____."

(5) "All distribution of this report is controlled. Qualified DDC users shall request through _____."

If the report has been furnished to the Office of Technical Services, Department of Commerce, for sale to the public, indicate this fact and enter the price, if known.

11. SUPPLEMENTARY NOTES: Use for additional explanatory notes.

12. SPONSORING MILITARY ACTIVITY: Enter the name of the departmental project office or laboratory sponsoring *(paying for)* the research and development. Include address.

13. ABSTRACT: Enter an abstract giving a brief and factual summary of the document indicative of the report, even though it may also appear elsewhere in the body of the technical report. If additional space is required, a continuation sheet shall be attached.

It is highly desirable that the abstract of classified reports be unclassified. Each paragraph of the abstract shall end with an indication of the military security classification of the information in the paragraph, represented as *(TS), (S), (C), or (U)*.

There is no limitation on the length of the abstract. However, the suggested length is from 150 to 225 words.

14. KEY WORDS: Key words are technically meaningful terms or short phrases that characterize a report and may be used as index entries for cataloging the report. Key words must be selected so that no security classification is required. Identifiers, such as equipment model designation, trade name, military project code name, geographic location, may be used as key words but will be followed by an indication of technical context. The assignment of links, roles, and weights is optional.